THE ROLE OF NEBULIZED KETAMINE IN PAIN MANAGEMENT IN THE EMERGENCY DEPARTMENT

Henna Ali; Jemer Garrido; Sergey Motov (Creighton Omaha, NE)

ABSTRACT

Background, Significance, and Hypothesis: Ketamine is a non-competitive N-methyl-D-aspartate/glutamate-receptor complex antagonist that reduces pain by diminishing central sensitization at the level of the spinal cord and central nervous system. Ketamine is traditionally administered intravenously (IV) and intranasally (IN). When administered via IV or IN routes in the Emergency Department (ED), ketamine has been shown to be effective in patients with acute traumatic and non-traumatic pain. However, these methods each pose their own challenges. The intravenous push dose is not always readily available. Subdissociative ketamine administered IN could leave an unpleasant sensation, leading adult ED patients to decline this method. Therefore, another non-invasive route of ketamine administration, such as inhalation via a breath-actuated nebulizer (BAN), is recently being explored. Exploring this avenue could potentially improve pain management access in both the ED and pre-hospital settings.The objective is to carry out a focused clinical literature review evaluating the role of nebulized ketamine in pain management within the emergency department (ED) and pre-hospital settings. This method of administration could provide comparable analgesic benefits improving patient comfort and compliance.

Methods: A comprehensive search was conducted using the PubMed database using the following MeSH terms "nebulized ketamine," "pain management," "acute pain," "emergency department," and "pre-hospital setting". The studies focused on the role of nebulized ketamine for pain management in the ED. Nine studies were selected based on inclusion criteria, encompassing randomized controlled trials, case series, and case reports. Data extracted included population characteristics, dosages, pain scores, adverse effects, and the need for rescue analgesics. Descriptive statistics were employed to analyze the data.

Results: The review included 264 participants who received nebulized ketamine at doses of 0.75 mg/kg, 1 mg/kg, and 1.5 mg/kg. The average baseline pain score was 7.9, which decreased to 3.6 at 30 minutes and 2.7 at 60 minutes post-administration, indicating significant pain relief. Moderate to severe adverse effects were observed in 9.0% of patients, and 9.3% required rescue analgesics.

Conclusion: Nebulized ketamine, administered via a breath-actuated nebulizer, is an effective and well-tolerated option for short-term acute pain management in the ED and pre-hospital settings. However, further research with larger and more diverse patient populations is needed to confirm these findings and explore long-term safety and efficacy.

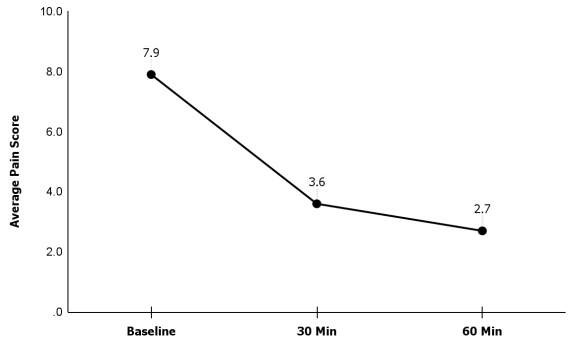

Figure 1: Average Pain Scores at Specified Time Points

TO ELUCIDATE THE ROLE OF PAX6/SOX2 AXIS IN ESTABLISHING BREAST CANCER BRAIN METASTASES

Laiba Anwar, Asad Ur Rehman, Mohammad Abbas Ali Zaidi, Parvez Khan, Mahek Fatima, Md Arafat Khan, Aatiya Ahmad, Nivedeta Krishna Kumar, Moorthy P Ponnusamy, Surinder K Batra, Juan A. Santamaria-Barria, Metin Uz, Mohd Wasim Nasser*

University of Nebraska Medical Center, Omaha, NE, USA.

Background, Significance, Hypothesis: Brain metastasis (BrM) remains the most severe complication of breast cancer (BC), the most diagnosed cancer in women, associated with an abysmal prognosis. Despite advances in cancer research, the molecular underpinnings that enable breast cancer cells to colonize and thrive in the brain remain poorly understood, creating a critical need for targeted therapeutic strategies. Our preliminary bioinformatics analysis of publicly available datasets revealed that Pax6, a transcription factor and a master regulator of transcription involved in normal development of the central nervous system (CNS) and eyes, was significantly upregulated in brain metastatic samples compared to primary breast tumors. Pax6 has previously been implicated in enhancing cancer cell proliferation, migration, and resistance to apoptosis in various cancers. Importantly, Pax6 regulates key stemness factors, including SOX2, OCT4, NANOG, and KLF4, which endow cancer cells the increased adaptability, self-renewal capacity, and latency- hallmark of metastatic progression and therapy resistance. Cancer stem cells, known for their tumor initiating potential are pivotal in the formation of metastatic lesions as well as the establishment of dormant states that evade the immune detection and therapeutic interventions. These stemness driven mechanisms are critical in sustaining breast cancer brain metastases (BCBrM). We hypothesize that Pax6 plays a central role in promoting cancer stem cell traits and latency in BCBrM, thereby driving disease progression and therapy resistance. By elucidating functional role of Pax6 in this context, we aim to identify therapeutic targets to mitigate the devastating effects of BCBrM and improve patient outcomes. Understanding these mechanisms will provide novel insights combating this aggressive and poorly understood disease.

Experimental Design: To test this hypothesis, we conducted a series of in vivo and in vitro experiments. For the in vitro phase, we used CRISPR/Cas9 to generate Pax6 Knockout (KO) in BCBrM cells and performed proliferation and migration assays. We also generated Pax6 overexpression (OE) in BC cell lines and performed migration and proliferation assays to see if Pax6 overexpression in primary cells would induce a BrM-like phenotype. Additionally, we performed side population analysis as well as mammosphere formation assay to confirm the stem cell characteristics of these BCBrM cells.

In the in vivo phase, we injected Pax6 KO and control cells intracardially into immunocompromised mice and observed the development of metastatic lesions in the brain over the course of 6-8 weeks.

Data and Results: In vitro results demonstrated that BCBrM cells with Pax6 KO had decreased proliferation, wound healing and migration properties. Conversely, overexpression of Pax6 in primary BC cells induced a BrM-like phenotype, enhancing proliferation, migration, and wound healing. Since Pax6 regulates stem cell features, we also found that Pax6 KO reduced the expression of stemness-promoting factors such as OCT4, NANOG, and KLF4. We also observed reduced expression of SOX2 in Pax6 silenced BCBrM cells. Moreover, Pax6 KO cells demonstrated significant reduction in mammosphere-forming abilities and side populations. In the in vivo studies, intracardiac injection of Pax6 KO BCBrM cells into immunocompromised mice resulted in a significant reduction of brain metastatic tumor lesions compared to controls.

Conclusion: The results support the hypothesis that the Pax6/Sox2 axis mediates stemness i and enhances the metastatic potential of BCBrM cells. The observed reduction in proliferation, migration, stemness characteristics, brain metastatic tumor burden in Pax6 KO cells highlights its importance as a therapeutic target. These findings highlight the novel role of Pax6 and Sox2 in promoting stemness in BCBrM cells and thereby enhance breast cancer brain metastasis.

EXPLORING THE MICROBIOME AND GUT-STEM CELL AXIS IN PANCREATIC DUCTAL ADENOCARCINOMA

Kirtana Arikath, Prabagaran Narayanasamy, Seoung-Ryoung Choi, Zahraa Wajih I Alsafwani, Annant Bir Kaur , Venkatesh Varadharaj, Nivedeta Krishna Kumar, Surinder K.Batra and Moorthy P.Ponnusamy

Department of Biochemistry and Molecular Biology, University of Nebraska Medical Center, Omaha, NE.

BACKGROUND: Pancreatic Ductal Adenocarcinoma (PDAC) is a highly aggressive malignancy with a survival rate of less than 10%. While genetic mutations have long been linked to cancer, emerging research highlights the microbiome's critical role in cancer initiation and progression. Microbes can promote inflammation, produce DNA-damaging toxins, and generate carcinogenic metabolites, making tumors more resistant to chemotherapy and immune responses. In PDAC, the tumor microenvironment (TME) is marked by a dysbiotic microbiome, along with cancer-associated fibroblasts (CAFs), immune cells, and cancer stem cells (CSCs). The degree of stress and inflammation in the surrounding microenvironment, brought on TLR AND NFKB
by the different additional components in the TME, is crucial for the maintenance of CSCs. It is thus reasonable to speculate that the microbiome is another essential factor influencing the evolution of CSCs.

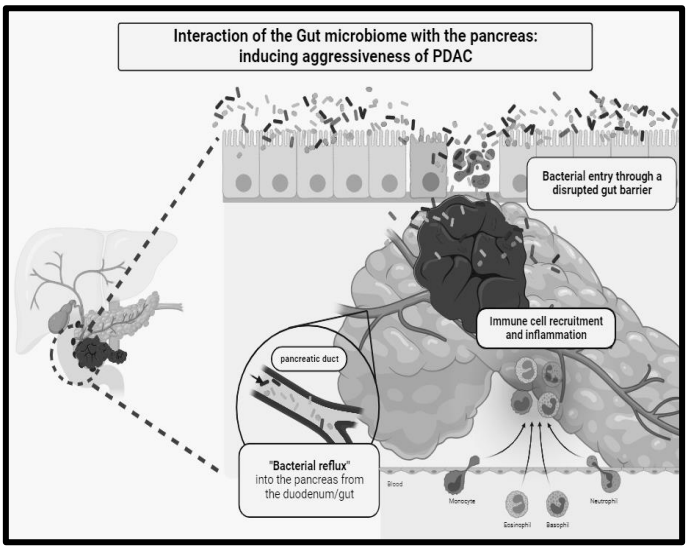

SIGNIFICANCE: Cancer stem cells (CSCs) play a pivotal role in metastasis, recurrence, tumorigenicity, and resistance to therapeutic interventions. The human body is host to a diverse array of microorganisms, including bacteria, fungi, and viruses, collectively known as the microbiome. Each organ has its distinct microbiome, with particular focus in recent research on the gut microbiome. In the context of pancreatic ductal adenocarcinoma (PDAC), the tumor microenvironment (TME) is often characterized by a dysbiotic microbiome, which may result from bacterial reflux from the gut through the pancreatic duct or the infiltration of gut-derived microorganisms into the pancreas due to a compromised epithelial barrier. This disrupted microbial balance can potentially establish a niche that supports the CSC population. Therefore, targeting and modulating the microbiome within the PDAC TME holds significant promise as a therapeutic strategy for improving patient outcomes.
HYPOTHESIS: The microbiome may play a crucial role in influencing the cancer stem cell population, thereby impacting the progression of PDAC.

EXPERIMENTAL DESIGN: We Analyzed the existence of bacteria using Lipopolysaccharide (LPS) staining on human and mouse PDAC samples along with dual staining of cancer stem cell markers. Fluorescent In-situ hybridization (FISH) was used to detect bacterial species in human and mouse PDAC and standard tissue samples. LPS treatment and treatment with bacterial supernatant and bacterial cell-free lysate with PDAC and regular pancreatic cell lines showed enrichment in particular cancer stem cell markers. This treatment established an environment where cancer cells are exposed to bacterial metabolites and toxins. A Co-culture model of three different bacterial species with mammalian PDAC and regular pancreatic cell lines was established to see enrichment in cancer stem cell maintenance by analyzing CSC gene expression through Immunofluorescence. An in vivo model was established by administering an oral antibiotic cocktail to KC*(K-ras$^{LSL.G12D/+}$;Pdx-1-Cre)* and KPC*(K-ras$^{LSL.G12D/+}$; Trp53$^{R172H/+}$; Pdx-1-Cre)* mice to investigate its impact on PDAC tumor development.

RESULTS/DATA: Analysis of publicly available datasets showed a disrupted microbiome in the basal-like subtype compared to the classical subtype of PDAC, along with differential expression of certain bacterial species**.** We observed gram-negative bacteria in human and mouse PDAC samples using Lipopolysaccharide staining. We also observed the dual expression of stem cell markers CD44 and LPS. The presence of bacterial species in PDAC and standard tissue samples from humans and mice was confirmed with Fluorescent In-situ hybridization of bacterial 16srRNA. In vitro, treatment of cells with LPS and bacterial supernatant showed specific enrichment of certain stem cell markers and proliferation markers. Co-culture of three different bacterial species *(Pseudomonas aeruginosa, Sphingopyxis macrogoltabida, Acinetobacter baumanii)* with mammalian PDAC cell lines enriched cancer stem cell markers, CD44 and Sox9.Administration of the antibiotic cocktail to KC*(K-ras$^{LSL.G12D/+}$;Pdx-1-Cre)* and KPC*(K-ras$^{LSL.G12D/+}$; Trp53$^{R172H/+}$; Pdx-1-Cre)* mice showed evidence of structural variation in PDAC.

CONCLUSION: Overall, our preliminary results validate our hypothesis, demonstrate the presence of bacteria in the PDAC TME, and shed light on the intricate connection between the gut microbiome and PDAC development, specifically through cancer stem cell population enrichment.

SYSTEMATIZED REVIEW OF SGLT2 INHIBITOR AND GLP-1RA USAGE IN ISOLATED LIVER TRANSPLANT RECIPIENTS

Marissa Baker[1], Mary Leick[2], Shaheed Merani[1], and Faruq Pradhan[1]
1- University of Nebraska Medical Center College of Medicine, Omaha, NE
2- Nebraska Medicine, Omaha, NE

Background, Significance, Hypothesis: Sodium-glucose cotransporter 2 (SGLT2) inhibitors and glucagon-like peptide-1 receptor agonists (GLP-1RAs) have benefits proven in the general population; however, their efficacy and safety in liver transplant recipients (LTRs) have not been well studied. The objective of this study was to evaluate the effect of SGLT2 inhibitors and GLP-1RAs on all-cause mortality, steatosis, immunosuppression, renal and CV function, and safety outcomes in LTRs.

Experimental Design: A systematized review was conducted utilizing EMBASE, MEDLINE, Scopus, and Cochrane Library databases with studies included between Jan 1, 2005, to May 12, 2024. Included studies investigated the usage of SGLT2 inhibitors or GLP-1RAs to treat pre-existing type 2 diabetes mellitus or post-transplant diabetes mellitus in solitary LTRs. Studies with limited reported data and non-English publications were excluded, along with animal and cell studies. The primary outcome was the effect on liver allograft endpoints, including steatosis, graft survival, and rejection. Secondary outcomes included changes in metabolic comorbidities, renal dysfunction, all-cause mortality, and incidence of major adverse side effects.

Data and Results: Five studies were identified, all published as conference abstracts. The incidence of graft failure was reported in only one study. There were no documented incidents of rejection. Weight decreased significantly with GLP-1RA use and trended downwards with SGLT2 inhibitor use along with improvement in HbA1c. No significant difference was seen across investigated secondary outcomes. The most common adverse event reported was gastrointestinal complaints with GLP-1RA use. No incidents of hypoglycemia, renal dysfunction, urinary tract infections, or pancreatitis were reported.

Conclusions: Overall, studies looking at GLP-1RA and SGLT2 inhibitor use in the LTR population are lacking. The limited data available is promising, especially in terms of weight loss without major adverse side effects or reported graft complications. Future studies will need to continue to investigate safety outcomes, especially the relationship between GI side effects and immunosuppressant levels.

ATP-DEPENDENT CHROMATIN REMODELING IN REGULATING DNA SECONDARY STRUCTURES

Sanjana Banerjee, Jim Persinger, Sandipan Brahma
University of Nebraska Medical Center, Omaha, NE

Background, Significance, Hypothesis: Guanine-quadruplexes (G4s) are secondary DNA structures composed of stacked G-tetrads, each containing four Hoogsteen hydrogen-bonded guanines in a planar arrangement. G4s have emerged as significant elements in the regulation of transcription and are frequently located in accessible regions of the genome. Their involvement in a variety of diseases, including cancers and neurodevelopmental disorders, highlights the critical need for precise genome-wide profiling of G4s as well as understanding their function and regulation.

Recent research has revealed that several ATP-dependent chromatin remodelers, including the mammalian SWI/SNF complex (BAF), are mapped to G4 genomic coordinates. These remodelers have been identified as strong G4-interactors through chemical mapping experiments. This suggests that G4s might play a crucial role in modulating ATP-dependent chromatin remodeling.

In our study, we aim to systematically profile G4 structures across the genome to functionally characterise their interactions with the BAF complex. This would allow us to gain new perspectives on mechanisms underlying gene regulation and their implications in disease.

We hypothesize that SMARCB1, a core subunit of the BAF complex, interacts with G4s to help recruit BAF to specific genomic loci. BAF in turn would evict nucleosomal histones to generate accessible chromatin required for the maintenance of G4 structures and active transcription.

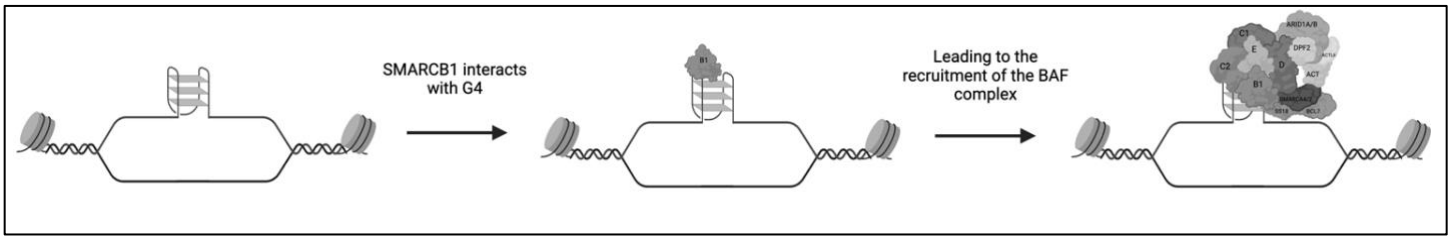

Proposed model: SMARCB1, a core subunit of the BAF complex, interacts with G-quadruplex (G4) structures to facilitate the recruitment of the BAF complex to specific genomic loci. This recruitment promotes nucleosome eviction, resulting in accessible chromatin that supports the maintenance of G4 structures and active transcription

Experimental Design: To test our hypothesis, we will perform CUT&RUN genome-wide mapping for G4s using a G4 specific antibody (BG4), and different BAF subunits upon G4 stabilization with pyridostatin (PDS). Additionally, we will determine the effects of acute depletion of BAF subunits such as SMARCB1 using a dTAG-based degron system, to determine their roles in BAF recruitment and stabilizing G4 structures.

Data and Results: Preliminary experiments using CUT&RUN to profile G4in mouse embryonic stem cells revealed enrichment of G4s broadly over all accessible chromatin that are also occupied by RNA Polymerase II. These sites also show enrichment of BAF subunits such as SMARCA4 and SMARCB1.

Conclusion: On comparing our preliminary data to already published data, it is evident that our CUT&RUN profiling data looks different compared to the ones available publicly. The profile indicates that the G4s are present in a more widespread manner in mouse embryonic stem cells. Additionally, enrichment of BAF subunits at these G4 structures indicates that the BAF complex is interacting with G4s. Further experiments would enhance our understanding of these interactions and help us dissect the functional relevance of it.

RACIAL DISPARITIES IN SYSTEMIC LUPUS ERYTHEMATOSUS (SLE) MORTALITY FROM 1999-2022

Joseph Bettag, Sagar Patel, Nikita Baral, Ali Bin Abdul Jabbar, Abubakar Tauseef (*Creighton University School of Medicine, Omaha, NE)*

Background, Significance, Hypothesis: Systemic lupus erythematosus (SLE) is a chronic autoimmune disease with variable mortality rates among different demographic groups. Despite treatment advancements, disparities in SLE outcomes continue to exist. To this day, no literature has been published investigating racial trends in SLE mortality using the CDC Wonder database. Additionally, very little has been published looking at how mortality was affected during the COVID-19 pandemic. We predict that non-Hispanic White population will have the lowest overall mortality rates over the study period while the Black population will have the highest rates.

Experimental Design: This study utilized CDC WONDER database data from 1999 to 2022 to examine SLE-related mortality trends. SLE deaths were identified using the International Classification of Diseases, 10th Revision, Clinical Modification (ICD-10-CM) codes M32.0 (Drug-induced systemic lupus erythematosus), M32.1 (Systemic lupus erythematosus with organ or system involvement), M32.8 (Other forms of systemic lupus erythematosus), and M32.9 (Systemic lupus erythematosus, unspecified). Age-adjusted mortality rates (AAMRs) were calculated with Joinpoint regression for trend analysis.

Data and Results: Over the study period, 50,458 SLE-related deaths occurred in the United States. The overall AAMR decreased from 1.18 per 100,000 in 1999 to 0.92 in 2022, with a notable decrease early in the study and an increase after 2013. The Black population had the highest AAMR throughout the study period, with an AAMR of 3.05 (95% CI 2.69 to 3.17) in 1999, followed by a decrease in AAMR to 2.22 (95% CI 2.09 to 2.45) in 2022, with an AAPC (average annual percent change) of -1.31 (95% CI -2.13 to -0.41). The Hispanic population also saw a reduction in AAMR from 1.53 (95% CI 1.07 to 1.40) in 1999 to 1.04 (95% CI 0.79 to 0.99) in 2022, with an AAPC of -0.54 (95% CI -1.48 to 0.42). The non-Hispanic White population had the lowest AAMR, starting at 0.84 (95% CI 0.84 to 0.94) in 1999 and decreased to 0.66 (95% CI 0.81 to 0.91) in 2022. The AAPC from 1999 to 2022 was -0.53 (95% CI -1.11 to 0.02). When these racial groups were stratified by gender, females of all races had higher AAMR's than males of all races. A similar pattern was observed with black females and males facing the highest AAMR's while white females and males facing the lowest AAMR's for their respective genders.

Conclusion: The findings of this study highlight the need for targeted public health interventions and policies to reduce inequalities and improve outcomes for individuals affected by SLE. Efforts to reduce these disparities could include increasing access to specialized care for high-risk groups, enhancing patient education about SLE management, and addressing the socioeconomic barriers that hinder effective treatment.

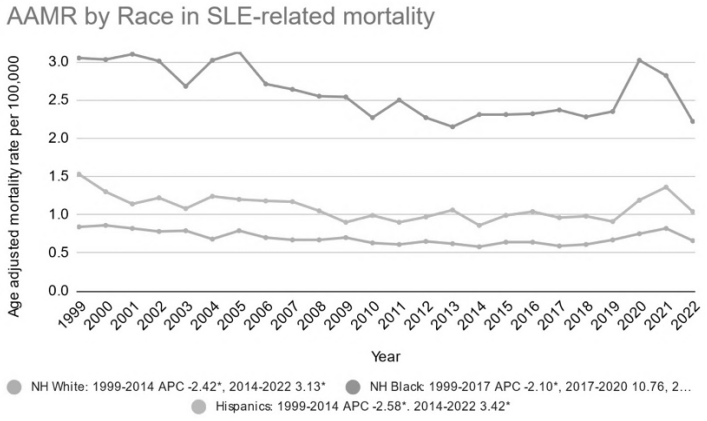

Figure 1. Age-adjusted mortality rates stratified by race/ethnicity in SLE-related mortality from 1999-2022 in the United States.

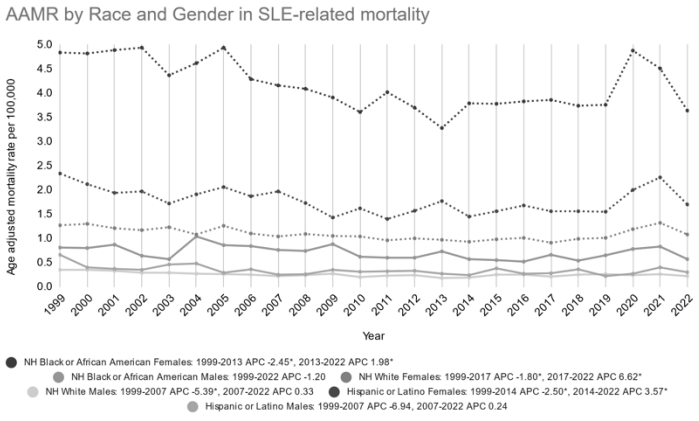

Figure 2. Age-adjusted mortality rates stratified by race/ethnicity and gender in SLE-related mortality from 1999-2022 in the United States.

NOVEL MECHANISMS OF TFEB NUCLEAR IMPORT AND EXPORT BY cAMP SIGNALING

Saumya Bhatt[1], Mohammad Ali Abbas Zaidi[1], Nicholas Woods[1], Micah B. Schott[1]
[1]University of Nebraska Medical Center, Omaha, NE

Background:
Transcription factor EB (TFEB) plays a key role in fatty liver disease by transcribing genes related to lysosome biogenesis, cellular energy homeostasis, and autophagy. TFEB activity depends on its cytosolic vs nuclear localization, which is mainly dictated by the phosphorylation/dephosphorylation of specific amino acid residues. TFEB can be phosphorylated at multiple serine residues by an array of different protein kinases, and phosphorylation can either inhibit or activate TFEB depending on the kinase and phosphorylation site. Intriguingly, analysis of TFEB's sequence identified a phosphorylation motif specific for cAMP-dependent protein kinase A (PKA) at serine 467 (RRxS). However, the impact of cAMP-PKA signaling on TFEB phosphorylation or cytoplasm-nuclear trafficking has not been studied. Therefore, we sought to elucidate the interplay between cAMP/PKA signaling and TFEB, focusing on its implications for subcellular localization and potential contributions to the pathophysiology of fatty liver disease.

Methods:
HeLa cells stably expressing TFEB-GFP were treated with cAMP agonists (10 μM Fsk + 0.5 mM IBMX) and/or the PKA inhibitor H89 (50 μM). TFEB subcellular localization was analyzed using nuclear-cytoplasmic fractionation followed by western blotting, and fluorescence microscopy. Further, to determine whether cAMP-dependent PKA is responsible for TFEB nuclear export, HeLa cells were treated with HBSS media to simulate amino acid deprivation, a condition known to promote TFEB nuclear translocation. After achieving maximum nuclear import of TFEB, the HBSS-treated cells were refed with regular media (amino acid-rich) to evaluate TFEB export under PKA-inhibited conditions. Phospho-proteomic analysis was performed to identify TFEB phosphorylation sites following cAMP-stimulation +/- the PKA inhibitor. Site-directed mutagenesis was also used to generate TFEB phospho-null (S467A) and phospho-mimic (S467D) mutants to validate phosphorylation effects on subcellular localization.

Results:
Activation of cAMP signaling induced rapid nuclear import of TFEB within 30 minutes, accompanied by enhanced lysosomal accumulation within 2 hours as indicated by Lysotracker staining. However, cAMP-induced nuclear import was transient, as TFEB was exported back to the cytoplasm between 2 and 8 hours after stimulation. Interestingly, inhibition of cAMP kinase (PKA) with H89 did not inhibit TFEB acute nuclear import but inhibited its downstream nuclear export. Notably, under conditions of PKA inhibition, TFEB shows increased nuclear retention 8-hours compared to the DMSO control. These findings suggest that while cAMP facilitates TFEB nuclear import, PKA activity is likely critical for nuclear export, potentially through a secondary mechanism. Phospho-mass spectrometry analysis of TFEB-GFP from HeLa cells treated with Fsk/IBMX revealed significantly increased phosphorylation of N-terminal serine residues (S109, S114, and S122) during the TFEB nuclear import phase (t=30 minutes). However, during the TFEB nuclear export phase (t=8h), phosphorylation of the C-terminal PKA-consensus motif (S647) was significantly elevated. This indicates that phosphorylation at S109, S114, and S122 is important for TFEB nuclear import, while PKA-dependent phosphorylation at S467 plays a key role in its nuclear export. Site-directed mutagenesis experiments support this claim, as the S467A mutant localizes predominantly in the nucleus, while the phosphomimic S467D mutant localizes primarily in the cytoplasm.

Conclusion:
cAMP/PKA signaling tightly regulates TFEB subcellular localization through distinct phosphorylation events. Our data are consistent with a model whereby cAMP facilitates acute and transient TFEB nuclear import and lysosomal biogenesis, while PKA-mediated phosphorylation at S467 is essential for nuclear export. These findings provide new insights into the cAMP-PKA-TFEB axis. Further studies are warranted to explore the functional consequences of these phosphorylation events on TFEB transcriptional activity.

CHARACTERIZATION OF IDENTIFIED NUCLEOPORIN PROTEINS IN CUTANEOUS SQUAMOUS CELL CARCINOMA

Aditi Charak, Moynul Islam, James A Grunkemeyer, Laura A Hansen

Background: Cutaneous squamous cell carcinoma (cSCC) is the second most common cancer in the United States, with approximately 90% of cases attributed to UV-induced mutations in basal keratinocyte cells within the epidermis. In a CRISPRi screen performed in our lab we identified six nucleoporin proteins whose knockdown caused a significant reduction in cell survival; including NUP62, NUP93, NUP98, RAE1, NUP160, and NUP214; suggesting they may be promising targets for therapy. Nucleoporins are proteins that constitute the nuclear pore complex. Based on their role in the nuclear pore complex, nucleoporins can either be classified under scaffold or FG-repeat nucleoporins. It is interesting to note that two of our identified nucleoporins are scaffold (NUP93 and RAE1) and two contain FG repeats and line the central channel (NUP62 and NUP98). In addition to nucleo-cytoplasmic shuttling of cargo, they are also important in gene regulation, and regulating cell growth and differentiation. This project was undertaken to evaluate the effectiveness of nucleoporin knockdown in induction of cell death of cSCC cells.

Significance: The multifunctional nature of nucleoporins as structural components of the NPC and their role in interacting with critical cargo molecules make them promising targets for therapeutic intervention in cSCC. Further research into these interactions could uncover new opportunities for targeted treatments.

Hypothesis: We hypothesize that CRISPRi-mediated knockdown of nucleoporin proteins NUP62, NUP93, NUP98, RAE1, NUP160, and/or NUP214 will reduce the survival of cSCC cells.

Experimental Design: Transfer plasmids containing a guide RNA sequence to target specific nucleoporins were prepared and used for lentiviral generation after transfecting into HEK293Ts with the recombinant transfer plasmids and the packaging and envelope plasmids. The lentiviral titre was determined prior to transduction of SCC-13 cSCC cells that expressed a dCas9 – KRAB domain followed by doxycycline treatment to induce knockdown. Knockdown of targeted proteins was validated by immunoblot. A resazurin assay was used to quantify how many cells remained viable after nucleoporin knockdown vs no knockdown.

Results: Lentiviruses containing guideRNAs specific for each nucleoporin were successfully produced and used to transduce the SCC13 cells. Validation of the knockdown of NUP62, NUP93, NUP98 and RAE1 in doxycycline(dox) induced vs un-induced SCC13 cells was confirmed by immunoblotting. Additionally, resazurin assays results indicated knockdown of NUP62 and NUP98 reduced cell viability.

Conclusions: NUP62 and NUP98 represent potential targets for cSCC treatment or prevention.

COMPARATIVE NUTRIENT STATUS OF CAROTENOIDS, RETINOL, AND TOCOPHEROL AMONG WIC PARTICIPANTS, INCOME-ELIGIBLE NON-PARTICIPANTS, AND HIGH-INCOME MOTHER-INFANT DYADS

Ridhi Chaudhary, Rebecca Slotkowski, Rebekah Rapoza, Corrine Hanson, Matthew VanOrmer, Melissa Thoene, Ann Anderson-Berry (UNMC Omaha, NE)

The Special Supplemental Nutrition Program for Women, Infants, and Children (WIC) is a federal initiative designed to improve the nutritional health of low-income families. WIC supports pregnant and postpartum women and young children, offering resources for healthy growth and development during the critical early years. Nutrients that are essential for growth and development include carotenoids and tocopherols which have antioxidant qualities.

Exploring the relationship between participation in the WIC program and levels of serum carotenoids, retinol, and tocopherols in mother-infant pairs is important for understanding the value of WIC in enhancing nutritional outcomes.

An IRB-approved study enrolled mother-infant pairs (n=232) at the time of delivery for collection of maternal and cord blood samples. At enrollment, 49 dyads (21.1%) were participants of the WIC program, 66 (28.4%) were income eligible, and 117 (71.6%) were part of the high-income control group. The Kruskal-Wallis test was used to assess differences in maternal and cord blood nutrient levels between WIC participants, income-eligible non-WIC participants, and the high-income control group. Data was adjusted for smoking status, corrected gestational age, and income to poverty ratio.

Data analysis of maternal blood samples showed no statistical significance in nutrient status amongst WIC participants, income-eligible participants, and the control group. Data showed statistically lower levels of α -carotene in the cord blood of WIC participating mother-infant pairs as compared to income-eligible participants (p=0.007) and the high-income control group (p=0.003) per table 1. The findings also showed lower levels of β -carotene in cord blood of WIC participating mother-infant pairs as compared to the control group (p=0.003). Lower levels of retinol were also observed in the cord blood of WIC participants as compared to the control group (p=0.019). In contrast, higher levels of γ-tocopherol were seen in cord blood of WIC participants as compared to the control group (p=0.038).

Interestingly, infants from low socioeconomic backgrounds whose mothers participate in the WIC program still exhibit poorer nutritional status compared to infants of mothers from higher-income groups. These findings have significant public health implications, as they shed light on the effectiveness of supplemental nutrition assistance programs for mothers and their infants. Future research will focus on evaluating additional factors, such as education, that may improve the diets of pregnant and postpartum women.

Table 1

Nutrient (µg/L)	WIC Participants	Income Eligible	Control Group	p-value
lutein + zeaxanthin	28.78 (18.44- 40.67)	32.02 (23.04- 48.46)	32.32 (24.32- 46.79)	0.266
β -cryptoxanthin	12.12 (8.03- 18.63)	13.91 (8.53-21.69)	12.93 (7.87- 22.42)	0.481
total lycopene	21.80 (15.71- 34.92)	26.59 (14.11-39.34)	22.15 (14.68- 34.67)	0.643
β-carotene	8.24 (4.87- 14.66)	9.88 (5.14- 24.27)	14.64 (7.85- 24.91)	0.003
α-carotene	2.80 (1.71- 4.48)	4.47 (2.95-8.93)	5.37 (2.29- 8.78)	0.002
retinol	162.15 (130.23- 237.49)	170.64 (135.32- 212.97)	201.19 (158.28- 261.37)	0.003
α -tocopherol	2085.74 (1466.47- 2958.34)	2629.26 (1694.72-3414.99)	2262.94 (1563.62- 3042.75)	0.158
γ -tocopherol	204.67 (113.39- 288.22)	181.75 (131.17- 244.39)	164.65 (72.65- 229.36)	0.020
δ -tocopherol	26.77 (12.19- 54.51)	23.34 (14.50- 61.10)	31.93 (14.24- 73.16)	0.477

SURVIVAL OUTCOMES ACROSS TREATMENT MODALITIES IN OROPHRYNGEAL SQUAMOUS CELL CARCINOMA

Kevin Choi, Elijah Torbenson, Nigel Lang, Peter T. Silberstein, John Paul Braun (Creighton SOM Omaha, NE)

Background: Oropharyngeal squamous cell carcinoma (OPSSC) is a malignant cancer with various treatment approaches, which can range from surgery or radiation to combination therapies. While multimodal treatments often produce better outcomes, survival differences between single and multimodal treatments remain underexplored. This study investigates the impact of treatment modality on survival outcomes, along with the influence of key demographic and clinical factors.

Significance of Problem: OPSCC treatment outcomes can be variable, and there is a need to evaluate the effectiveness of different treatment modalities to help guide clinical decision-making. Looking into 2022 compiled data from the National Cancer Database (NCDB), this study provides insights into the survival benefits of single and multimodal treatment strategies, contributing to the optimization of therapeutic approaches.

Hypothesis: How do different treatment modalities impact overall survival when adjusted for demographic and clinical covariates? This study hypothesizes that multimodal treatments are associated with superior survival outcomes in OPSCC when compared to single-modality treatments.

Experimental Design: The NCDB was used to identify patients diagnosed with OPSCC from 2004 to 2022. Cox proportional hazards regression assessed the relationship between treatment modality (observation, radiation, chemotherapy, surgery, and combinations) and survival, adjusted for covariates such as sex, age, Charlson-Deyo comorbidity score, and tumor stage. Kaplan-Meier survival curves and pairwise log-rank tests compared survival probabilities across groups. Mean and median survival times were also calculated. Analyses were performed on SPSS ver. 29.0.2.0, and statistical significance was set at $\alpha = 0.05$.

Results/Data: 1,652 patients were analyzed, and the most common treatment modality was radiation combined with chemotherapy (51.2%), which was followed by radiation-only (11.7%). Observation was associated with a significantly lower hazard of death (HR = 0.643, $p = 0.037$) with a mean survival time of 19.127 months, while chemotherapy-only demonstrated a significantly high hazard of death (HR = 2.350, $p < 0.001$) with the lowest mean survival time of 18.382 months. Surgery combined with radiation demonstrated the second longest mean survival time of 31.176 months with the highest significant hazard of death (HR = 2.657, $p < 0.001$). Older age (HR = 1.022, $p < 0.001$), higher Charlson-Deyo scores (HR = 1.268, $p < 0.001$), and advanced stage (HR = 1.114, $p < 0.001$) were independently associated with worse outcomes.

Conclusions: This study highlights the critical role of patient selection in determining the most appropriate treatment modalities for OPSCC. At first glance, the results for hazard of death and mean survival time for chemotherapy-only, as well as those for surgery combined with radiation, appear contradictory. However, these findings underscore the nuanced importance of patient selection. Patients receiving chemotherapy alone are often in more advanced stages of disease and treated palliatively, leading to worse outcomes compared to observation. The high hazard of death but long mean survival time for surgery combined with radiation suggest a similar twist. While many patients in this group experienced poor outcomes, suggested by the high hazard of death, a subset of patients derived significant benefit from the treatment, which is indicated by the long mean survival time. These results emphasize the need for individualized treatment planning to optimize survival outcomes and highlight the importance of further research into the factors influencing treatment selection and its impact on outcomes.

IN VITRO ADME, MOUSE PHARMACOKINETICS, AND BIOANALYSIS OF LD14b: A NOVEL Aβ 17β-HSD10 MODULATOR FOR THE TREATMENT OF ALZHEIMER'S DISEASE

Sohel Daria, Devendra Kumar, Nagsen Gautam, Jawaher Abdullah Alamoudi, Louise F. Dow, Paul C. Trippier, and Yazen Alnouti (UNMC Omaha, NE)

Background, Significance, Hypothesis: LD14b is an amyloid-β (Aβ) 17β-hydroxysteroid dehydrogenase type 10 (Aβ-17β-HSD10) protein-protein interaction modulator that shows promising *in vitro* and *ex vivo* activity to rescue Aβ-induced mitochondrial dysfunction, Aβ-induced toxicity, and Aβ-mediated inhibition of estradiol synthesis.

Experimental Design: The current study investigated *in vitro* human S9 fractions metabolic stability, apparent permeability across Caco-2 cells monolayer, human and mouse plasma protein binding, *in vivo* pharmacokinetics, and tissue distribution in Balb/cJ mice.

Data and Results: A fast, sensitive, reliable, and reproducible LC-MS/MS method was developed and validated over the dynamic range of 1-1000 ng/mL for the quantification of LD14b in different biological matrices (plasma, liver, kidney, brain, lungs, heart). LD14b was metabolically stable in human liver S9 fractions with 70% remaining after 90 minutes of incubation. It had intermediate apparent permeability of 3.55×10^{-06} cm/s and 6.16×10^{-06} cm/s for apical-to-basolateral (A-to-B) and basolateral-to-apical (B-to-A), respectively across the Caco-2 monolayer, and was medium/highly bound to human plasma proteins (84.1%), mouse plasma proteins (85.7%). LD14b had a 52% oral bioavailability in Balb/cJ mice and was well-distributed to the peripheral tissues (liver, kidney, lungs, and heart) including the brain. Orally, maximum plasma concentration (1780±131.6 ng/mL) was achieved in 0.45 h with a half-life of 3.8 h, a clearance 3.65 L/h/kg. About 5-7 folds higher brain concentration of LD14b was found compared to plasma concentration.

Conclusion: In conclusion, these results support the further development of LD14b as a potential therapeutic modality for Alzheimer's disease via oral administration.

IDENTIFICATION OF INTERACTING GENETIC RISK FACTORS FOR HEREDITARY CANCER USING SANGER SEQUENCING DATA AND PEDIGREE ANALYSIS

Olivia Doll, Holly Stessman, Cynthia Watson (Creighton University School of Medicine Omaha, NE)

Background, Significance, Hypothesis: Approximately 5-10% of cancers are hereditary, and several hereditary cancer syndromes characterizing genetic risk factors have been identified. While surveillance and prophylactic measures have been shown to improve outcomes for at-risk individuals, known genetic risk factors do not account for all cases of hereditary cancer. Although DNA repair genes *BRCA1* and *BRCA2* were until recently the only genes screened when evaluating patients for hereditary breast ovarian cancer (HBOC), mutations in these genes are only associated with 20-25% of HBOC cases. This project takes advantage of the Henry Lynch Memorial Biobank, an untapped resource of families with suspected hereditary cancer, ideal for tracing how specific variants contribute to cancer and how multiple variants within a family interact with each other to exacerbate cancer risk. Analyzing the interactions between multiple genetic risk factors in families with hereditary cancer will be helpful not only for counseling families about their level of risk, but also for understanding the molecular mechanisms of carcinogenesis, and for developing new targeted treatments.
Experimental Design: Individuals were screened for variants in 58 known cancer associated genes using MIPgen, a targeted molecular inversion probe sequencing approach. Families with inherited *BRCA1* and *BRCA2* variants were then evaluated for additional variants of interest. Each variant's pattern of inheritance and each affected family member's outcome was traced using pedigree analysis.
Results: Three individuals in family 1 shared a known pathogenic Chek2 missense variant. Two of these three individuals had additional risk associated variants in *ATM* and *POLD1*, respectively. 33 individuals in family 2 shared a pathogenic *BRCA2* stop gain variant. Two individuals had a missense variant in RAD50 in addition to the familial *BRCA2* variant and one individual had the same *RAD50* variant in the absence of the familial *BRCA2* variant. Two individuals shared a *FANCM* missense variant, one of whom also carried the familial *BRCA2* variant.
Conclusions: Siblings 15, 22, and 27 in family 1 shared a *CHEK2* variant associated with Li Fraumeni syndrome, prostate, breast, ovarian, colorectal, gastric, and adrenal cortex carcinoma, and osteosarcoma. Individual 27 was diagnosed with colorectal cancer at age 78 and carried an additional missense variant of undetermined significance (VUS) in *POLD1*, a gene associated with increased risk of colorectal cancer. There have been no reports of *CHEK2* and *POLD1* interacting or influencing an individual's cancer risk nor outcome. Individual 15 was diagnosed with pancreatic cancer at 97 and had an *ATM* VUS in addition to the *CHEK2* variant shared with his siblings. Although *ATM* and *CHEK2* participate in the same S phase checkpoint regulation pathway, the patient's presentation late in life with a cancer associated with neither of these mutations reduces the likelihood that either mutation or their combination contributed to his cancer diagnosis. Curiously, the third sibling to carry the *CHEK2* variant, 22, was never diagnosed with cancer. Three additional siblings for whom samples were not available were diagnosed with pancreatic cancer at ages 45 and 64 and gallbladder cancer at age 61, respectively. In family 2, in addition to a known pathogenic stop gain *BRCA2* variant, one affected individual, 360, who was diagnosed with breast cancer at 36, was found to carry a *FANCM* missense variant. Her sister, 357, was diagnosed with breast cancer at age 51, and carried only the *FANCM* variant. *FANCM* and *BRCA2* code for two of the thirteen Fanconi Anemia proteins. Three additional FA genes (*FANCD1, FANCJ,* and *FANCN*) have been identified as breast cancer susceptibility genes, and *FANCM* has been associated with triple negative breast cancer. Two different affected individuals, mother 280, who was diagnosed with breast cancer at 59, ovarian cancer at 71, and lobular breast cancer at 72 and daughter 282, who was diagnosed with breast cancer at 53 and lobular breast cancer at 65 shared both the familial *BRCA2* variant associated with hereditary breast and ovarian cancer as well as a missense variant in *RAD50,* a double strand break repair gene. 280's daughter, 285, carried only the *RAD50* variant and was diagnosed with ovarian cancer at 58. *RAD50* is known to be part of the *BRCA1* associated genome surveillance complex, which senses structurally aberrant DNA and regulates postreplication repair. *RAD50* mutations have been associated with poorer outcomes in breast cancer patients, suggesting an interaction that should be explored. In these groups with additional variants, individuals with multiple variants had earlier ages of onset or less severe diagnoses, supporting the hypothesis that mutations in multiple cancer associated genes interact to increase an individual's risk of developing cancer. Further research is warranted to better understand these interactions. Future directions include analysis of whole genome sequencing data from families in the biobank, including family 1 from this study.

TRENDS IN ACUTE MYOCARDIAL INFARCTION AND CEREBRAL INFARCTION MORTALITY IN THE UNITED STATES: A CDC WONDER STUDY FROM 1999-2022

Caroline Doyle, Gloria Jung, Taylor Billion, Vikram Murugan, Abubakar Tauseef, MD (Creighton University School of Medicine Omaha, NE).

Background, Significance, and Question: Acute myocardial infarction (MI) and cerebral infarctions are significant causes of mortality in the United States. Thus, understanding the trends in overall mortality over time is crucial for improvement of health outcomes. Our question was how mortality would change from 1999 to 2022 as determined from a free public health database.

Experimental Design: Our study extrapolates relevant data from the Center for Disease Control and Prevention (CDC) WONDER database. We use this to look specifically at the age-adjusted mortality rates (AAMRs) and annual percentage changes (APCs) over time, stratified by gender. Values were calculated using a multiple Joinpoint regression model.

Results/Data: From 1999 to 2022 there were 25,244 deaths due to acute myocardial infarction (MI) and cerebral infarction in the United States. Over this time period, the overall age-adjusted mortality rates (AAMR) decreased from its highest value of 1.65 (95% CI 1.57 to 1.73) in 1999 to its lowest value of 0.52 (95% CI to 0.47 to 0.56) in 2013. This then increased back to 1.25 (1.19 to 1.3) in 2022. There was an average annual percentage change (AAPC) of -1.6761 (95% CI -2.3861 to -0.9159) (Figure 1). The annual percentage change (APC) in AAMR was -10.5156 (95% CI -12.98486 to -8.7903) from 1999 to 2011, which increased to 8.9656 (95% CI 6.6793 to 12.4575) from 2011 to 2022 (Figure 1).

The AAMR decreased in males from its highest value of 2.06 (95% CI 1.91 to 2.21) in 1999 to its lowest value, 0.61 (95% CI 0.54 to 0.68) in 2011. The AAMR then increased back to 1.59 (95% CI 1.49 to 1.69) in 2022. The AAPC from 1999 to 2022 was -1.0604 (95% CI -1.6753 to -0.4131) (Figure 1). The APC in AAMR increased from 1999 to 2012 when it was -10.2473 (95% CI -12.232 to -8.7838) to 12.23026 (10.0974 to 15.348) from 2012 to 2022 (Figure 1). In females, the AAMR decreased from its highest value 1.42 (95% CI 1.33 to 1.52) in 1999 to its lowest 0.42 (95% CI 0.37 to 0.47) in 2013. The AAPC from 1999 to 2022 was -1.9664 (95%CI -2.8517 to -1.1313) (Figure 1). The APC in AAMR increased from 1999 to 2011 where it was -10.9311 (95% CI -13.904 to -9.0182) to 8.8454 (95%CI 6.0381 to 12.7774) (Figure 1).

Conclusions: This study provides perspective on the evolving trends for two increasingly pertinent health concerns, acute myocardial infarction (MI) and cerebral infarction. The initial decrease, followed by increase is intriguing and suggests potential gaps in care for patients with co-morbid conditions. Additionally, our study contributes to the growing body of literature exemplifying the profound medical research utility in stratifying national data banks such as CDC WONDER.

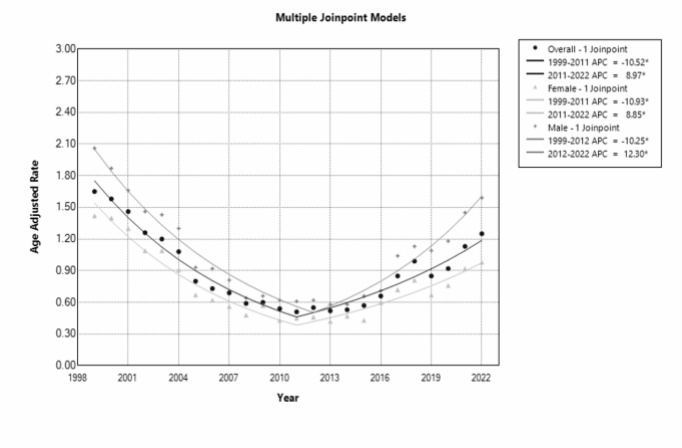

Figure 1. Joinpoint model of MI and cerebral infarction-related AAMR per 100,000 people overall and stratified by gender, 1999-2022 (*indicates the APC is statistically significant).

OSTEORADIONECROSIS OF THE HYOID BONE: A SYSTEMATIC REVIEW

Quentin H. Drane, Andrea Ziegler, Eric J. Thorpe (Creighton University School of Medicine, Omaha, NE)

Background, Significance, Problem: Radiation therapy (RT) plays an essential role in the treatment of several head and neck cancers; and despite technological improvements in radiation techniques, several adverse effects remain prevalent. Osteoradionecrosis (ORN) is among the most serious complications following RT for head and neck malignancies. With a prevalence of around 8%, it most commonly affects the mandible. Significant research has been performed to assess risk factors and disease progression of mandibular ORN and to improve its recognition and management. However, extra-mandibular ORN, particularly that of the hyoid bone, is less commonly reported and poorly understood. With the projected increase in the overall prevalence of oropharyngeal cancer in the coming decades, and an increasing number of reports of this unique complication, this study aims to provide a current perspective on clinical characteristics, radiologic findings, treatment modalities, and patient outcomes, as well as individual risk factors that may contribute to the development and severity of hyoid bone ORN.

Experimental Design: A comprehensive literature review of hyoid bone ORN was performed through PubMed and Scopus leading to the inclusion of 16 articles after our inclusion and exclusion criteria were applied. Patient variables, tumor characteristics, clinical presentation, and treatment variables were collected.

Data and Results: This study retrieved a total of 40 cases of hyoid bone ORN. The average age of patients was 60.0 years. The majority of patients were male (87.5%), and the majority of primary tumors were located in the oropharynx (77.5%). The average dose of RT was 66.2 Gy, and the average time between RT and hyoid bone ORN detection was 27.6 months.

The most common presenting symptom of hyoid bone ORN was dysphagia with or without concurrent odynophagia (16/40; 40.0%). Other signs and symptoms included non-specific neck pain, infection/inflammation, acute airway compromise, and otalgia (14/40; 35.0%, 8/40; 20%, 7/40; 17.5%, and 7/40; 17.5%, respectively).

Radiologic findings on CT imaging included cortical disruption or pathologic fracture of the hyoid bone, soft-tissue erosion or ulceration, and air- or fluid-filled pockets within or surrounding the hyoid bone. MRI demonstrated low signal intensity of the hyoid on T1 weighted images (T1WI) and mixed or high signal intensity on T2 weighted images (T2WI). PET-CT demonstrated increased metabolic activity in the hyoid bone in most patients (7/9; 77.8%) with an average standard uptake value (SUV) of 9.3.

Most patients with hyoid bone ORN were managed with multiple medical therapies or a combination of surgical and medical therapies (21/40; 52.5%). The most common pharmacological treatment was antimicrobials (13/40; 32.5%). In addition, about one-third of patients underwent surgical resection or removal of the necrotic hyoid bone (13/40; 32.5%). A significant number of patients required tracheostomy and tube feeding (12/40; 30% and 10/40; 25%, respectively).

Patients receiving concurrent radiation and chemotherapy were more likely to need surgery compared to those treated with RT alone (80% vs 30%, p=0.0042).

Conclusion: Hyoid bone ORN is a rare complication following radiation treatment of head and neck cancer. However, with the increasing rates of oropharyngeal cancers, hyoid bone ORN may be seen more often. Clinicians should be aware of the potential presenting symptoms and complications from this diagnosis and be familiar with thorough work-up and treatment.

IN THE QUEST FOR A HYPERACTIVE CHROMATIN REMODELER

Min Sze Ewe, Jim Persinger, Sandipan Brahma
University of Nebraska Medical Center, Omaha NE

Chromatin accessibility is central to regulating gene expression. ATP-dependent chromatin remodelers such as SWI/SNF play essential roles in creating and maintaining accessible chromatin regions to facilitate the binding of transcription factors and RNA Polymerase II (RNAPII), thereby being pivotal in regulating gene expression. In this project, we focus on the mammalian SWI/SNF complex also known as BRG1/BRM associated factor (BAF).

BAF regulates chromatin structure by repositioning and evicting genomic nucleosomes. BAF is also known to oppose the functions of Polycomb Repressive Complexes (PRC) at transcriptionally repressive genomic regions.
Consistent with its critical role in regulating chromatin structure and gene expression, subunits of the BAF complex are mutated in more than 20% of cancers. While most of these mutations result in a defective BAF complex (loss of function, LOF), cancer-associated mutations found within a specific domain (post-HSA) in the catalytic BRG1 subunit have been found to be biochemically gain-of-function (GOF), and genetically dominant.

Our previous work showed that BAF along with RNAPII dynamically probes both transcriptionally active and Polycomb-repressed chromatin. However, BAF is only able to evict nucleosomes to generate accessible chromatin at transcriptionally active regions with the help of transcription factors, while its function at Polycomb-repressed chromatin is abortive. Intriguingly, the post-HSA domain is known to be a negative regulator of BAF ATPase activity. **We hypothesize that cancer-associated mutations in the post-HSA domain relieves this negative regulation and converts the abortive probing mechanism of BAF at Polycomb-repressed chromatin regions into productive nucleosome eviction resulting in erroneous transcription activation.**

To test our hypothesis, we ectopically expressed BRG1 with a deletion of the post-HSA domain (∆postHSA) in mouse embryonic stem cells (mESCs) using lentiviral transduction. We then induced ∆postHSA expression with 2ug/ml of Doxycyline and harvested cellsthemlthemlthemethemat different time-points. Following that, we used Western blot to verify the inducible expression levels of our mutant BRG1 and genomics assays to determine chromatin changes upon ∆postHSA expression. We are performing the Cleavage Under Targets and Tagmentation (CUT&Tag) assay to determine genome-wide changes in the occupancy of BRG1, Polycomb complexes (PRC1 and PRC2), and histone post-translational modifications (PTM). Additionally, we will conduct Cleavage Under Targeted Accessible Chromatin (CUTAC) assay targeting BRG1 to map changes in chromatin accessibility upon ∆postHSA expression. Lastly, we will determine changes in nascent transcription via Precision nuclear Run-On Sequencing (PRO-seq).

This is an ongoing project. Our preliminary CUT&Tag data showed a downregulation of H3K27me3 (Histone PTM deposited by PRC2) at Polycomb Repressed promoters suggesting that there is increased nucleosome remodeling by BAF at these regions, consistent with our hypothesis.

CHARACTERIZATION OF THE OMEGA SUBUNIT OF BORRELIA BURGDORFERI'S RNA POLYMERASE

Shane Fleming[1] and Travis J Bourret[1],
[1]Creighton University, Omaha, Nebraska

Background, Significance and Hypothesis: Lyme disease is the most common vector borne disease in the U.S becoming more frequent where recently the CDC estimated 476,000 cases each year based on insurance records. It is caused by bacteria *Borrelia burgdorferi* which is transmitted by *Ixodes scapularis and Ixodes pacificus* across the United States. As *B. burgdorferi* cycles between tick to host, it encounters numerous environmental changes such as shifts in pH, organic acids, and osmolarity levels. *B. burgdorferi* successfully adapts to these environmental cues through changes in gene expression carried out by RNA polymerase (RNAP). The RNAP holoenzyme is comprised of two α subunits, a β subunit, and a β' subunit. Additional proteins have been implicated in the function of RNAP including RpoZ (i.e. omega subunit). Investigations of RpoZ homologues from other bacteria have suggested the omega subunit helps stabilize the RNAP holoenzyme during gene transcription. Open reading frame *bb0820* of the *B. burgdorferi* genome is annotated as *rpoZ*, however, its function has yet to be tested. The goal of this study was to determine the functional role of RpoZ in *B. burgdorferi*. This is significant because RpoZ likely plays a critical role in the ability of *B. burgdorferi* to complete its infectious cycle and cause Lyme disease. My overarching hypothesis is RpoZ contributes to *B. burgdorferi* gene expression, growth, survival, and infectivity.

Experimental design: To test this hypothesis, I generated a suicide vector to knock out *rpoZ* from the *B. burgdorferi* chromosome. To confirm that the knockout was successful, I screened for the *rpoZ* gene and *rpoZ* expression using PCR, qPCR, and RNA sequencing. Successful transformants were also screened for possible plasmid *B. burgdorferi* 's 21 endogenous plasmids to verify use in subsequent experiments. Additionally, I performed RT-qPCR screening of genes adjacent to the *rpoZ* ORF to test for polar effects of the mutation of rpoZ. To test whether *rpoZ* contributes to growth, various growth curves and plating assays were performed. Growth curves were conducted using BSK II media at pH 7.6 and tested in different conditions that mirror growth in either tick vector or mouse host. Growth curves compared wild type *B. burgdorferi* vs the Δ*rpoZ* strain in a control experiment, varying acetate, osmolarity, and nutrient levels. Susceptibility assays were also performed comparing the growth of our wild type and *rpoZ* knockout strains after 2 hours of exposure to varying levels of hydrogen peroxide(H_2O_2) and the nitric oxide donor diethylamine NONOate (DEANO).

Data and Results: A successful knockout of *rpoZ* was confirmed by PCR, qPCR, and RNA sequencing. The transformant that had lost the least number of plasmids which was two was used for subsequent experiments. In the growth curve comparing wild type *B. burgdorferi* and the Δ*rpoZ* strain, when started at 1 x 10^5 cells ml^{-1}, WT reached mid log phase (1 - 5 x 10^5 cells ml^{-1}) after 3 days whereas Δ*rpoZ* reached mid log after 6 days. Varying acetate, osmolarity, and nutrient levels caused the Δ*rpoZ* to reach mid log phases at slower times compared to control BSK II. High osmolarity (600 mOsm) inhibited the growth of the Δ*rpoZ* strain showing RpoZ promotes resistance to osmotic stress. Similarly, the Δ*rpoZ* strain was hypersusceptible to oxidative stress as shown by a 4-log difference reduced survival of the Δ*rpoZ* strain compared to the WT after 2 hours of exposure to 0.5 mM H_2O_2. RNA sequencing showed 477 differentially expressed genes in the Δ*rpoZ* strain compared to wild type with many genes on the chromosome being downregulated and genes on plasmids upregulated.

Conclusion: Collectively, these data show RpoZ contributes to *B. burgdorferi*'s gene expression, growth, and survival. Further DNA and RNA analyses will be performed to elucidate the impact of RpoZ on *B. burgdorferi* mutation rate and growth defects, along with its contribution to the *B. burgdorferi*'s ability to infect ticks and mammalian hosts.

SEVERE ANEMIA CAUSES NEUROINFLAMMATION IN MURINE PUPS AND DISPLAYED IMPAIRED NEURODEVELOPMENTAL OUTCOMES IN ADULTHOOD

Juanitaa George Raj, Arjun Subrramanya, Balamurugan Ramatchandirin, Marie Amalie Balamurugan, Megan Ferris, Zainab D Lawal, Lauren Jantzie and Krishnan MohanKumar (UNMC Omaha, NE)

Background:

One in ten infants born in the United States are pre-term infants. Phlebotomy-induced anemia (PIA) is universal and variable in degree among preterm infants and may contribute to neurodevelopmental risk. In mice, PIA causes brain tissue hypoxia, however, the effects of severe anemia on brain neuroinflammation and potential neurodevelopmental outcomes remain largely unexplored.

Significance of the problem:

Anemia significantly impacts neurodevelopment and cognitive outcomes, affecting motor skills, emotional well-being, cognitive abilities, and educational performance.

Hypothesis:

Severe anemia-induced hypoxia leads to inflammatory changes in the neonatal mouse brain model of PIA and contributes to neurodevelopmental deficits during adulthood.

Experimental Design:

C57BL/6 mouse pups were studied in 2 groups (n=6 each): (1) naïve controls; (2) anemic (hematocrit 20-24%). Severe anemia was induced by facial vein phlebotomy on postnatal day (P) 2, 4, 6, 8, and 10. After 24 hours, whole brain tissue was subjected to qRT-PCR and Luminex Multiplex Assay for quantifying inflammatory cytokine expression and chemokine levels. Flow cytometry was performed to identify the microglial activation with triggered myeloid receptor-1 (*trem1*) expression. Untreated severe anemic mouse pups were allowed to grow until 12 weeks or 20 grams of body weight then touchscreen testing was performed to study the cognitive and behavioral realms.

Results:

We identified severe anemia contributes to hyper-inflammatory activation in the brain which was evident from significantly increased mRNA and protein expression of IL1α, IL1β, IFN-γ, IL6, and TNF-α. We have also found that levels of the chemokines (C-C motif ligands) MCP1 [CCL2], MIP1-α [CCL3], MIP1-β [CCL4], CXCL10 were also significantly increased in anemic mouse pups compared to control. Anemic-derived microglial cells showed strong immunoreactivity to the activation marker, P2RY12, and also expressing *trem1* indicates the microglial activation during anemia. The cognitive performance on visual discrimination (VD) assay showed only 32% of anemic mice were able to perform VD compared to 72% of control. Moreover, the number of errors throughout the visual discrimination paradigm was noted in anemic mice and had comparable reaction time and magazine latency throughout the VD paradigm. Anemic mice showed significantly impaired reversal learning, specifically only 20% of anemic mice passed the criteria for VD and reversal compared to 58.8% of control. Notably, anemic mice required more correction trials than control group.

Conclusions: Severe anemia leads to microglial activation-associated brain inflammation in murine neonates and persistently leads to impaired neurodevelopmental outcomes in their adulthood.

CCL21 THERAPY IN CONJUNCTION WITH LOW-DOSE METRONOMIC CYCLOPHOSPHAMIDE GENERATES SUPERIOR RESPONSES AGAINST NEUROBLASTOMA IN VIVO

Benjamin Gephart, Gabrielle Brumfield, Donald W. Coulter, and Joyce C. Solheim (UNMC, Omaha, NE)

Background, Significance, and Hypothesis: Neuroblastoma is a pediatric malignancy that arises from aberrant neural crest progenitor cell division and proliferation. Relapsed and refractory disease often has a poor prognosis, with the long-term survival rate less than 30%. Neuroblastoma is canonically considered to be an immunologically cold and non-immunogenic tumor type, with dense populations of immune suppressive cell populations that have been shown to impair anti-tumor immunity. Despite the significant clinical response in other tumor types, immune checkpoint inhibitors have only shown limited clinical efficacy in neuroblastoma. Superior treatment modalities are needed to increase overall survival with less severe toxicity in the treatment of neuroblastoma. CCL21 is a chemokine that mediates the migration of immune cell populations such as T cells, NK cells, and dendritic cells, which are key immune cell populations for robust anti-tumor immunity. Prior preclinical studies have highlighted the effectiveness of CCL21 therapy as a potential treatment modality for multiple solid tumor types; however, CCL21's effectiveness against neuroblastoma is poorly understood. We sought to investigate the effectiveness of intratumoral delivery of CCL21 therapy against neuroblastoma in vivo. We desired to also characterize the immunomodulatory properties of the alkylating agent cyclophosphamide against neuroblastoma both in vitro and in vivo. Cyclophosphamide is part of the standard-of-care treatment protocol for neuroblastoma and has been shown to possess unique immunomodulatory properties at low doses. Prior preclinical studies of both solid and hematologic malignancies have demonstrated synergy between immunotherapy and chemotherapy. Multiple chemotherapeutic agents have been shown to trigger immunogenic cell death capable of augmenting immune cell activation and infiltration. Consequently, we hypothesized that a dual treatment of in situ delivery CCL21 therapy in conjunction with low-dose metronomic cyclophosphamide will synergize to create superior antitumor immunity against neuroblastoma in vivo.

Experimental Design: Using an immunocompetent, syngeneic A/J mouse model, we evaluated the efficacy of a dual treatment of in situ delivered CCL21 therapy in conjunction of low-dose metronomic cyclophosphamide in controlling tumor growth and extending survival in Neuro2a tumor-bearing A/J mice. Our in vitro studies characterizing the effect of low-dose cyclophosphamide on cell surface calreticulin expression and PD-L1 expression were performed by culturing Neuro2a cells for 24 or 48 hours in low doses of cyclophosphamide followed by Neuro2a cell isolation, harvesting, and staining for flow cytometry analysis.

Data and Results: Herein, we demonstrate that CCL21 therapy in conjunction with metronomic low-dose cyclophosphamide chemotherapy generates superior controlling of neuroblastoma tumor growth in an immunocompetent, syngeneic Neuro2a mouse model relative to CCL21 alone or cyclophosphamide alone. CCL21 in conjunction with low-dose metronomic cyclophosphamide was more effective in controlling tumor growth in the latter phase of study, further supporting our hypothesis of synergy in potentiating long-term anti-tumor immunity. In our in vitro studies, we show that low-dose cyclophosphamide up-regulates cell surface calreticulin expression, as well as cell surface PD-L1 expression on neuroblastoma tumor cells, suggesting that it has potential to facilitate sensitization to anti-PD-L1 checkpoint blockade.

Conclusion: In short, this research shows the therapeutic potential of CCL21 therapy and metronomic low-dose cyclophosphamide chemotherapy in the treatment of non-immunogenic tumor types such as neuroblastoma. Furthermore, this research supports the technical feasibility of a novel in situ tumor immunotherapy strategy for neuroblastoma in a preclinical setting.

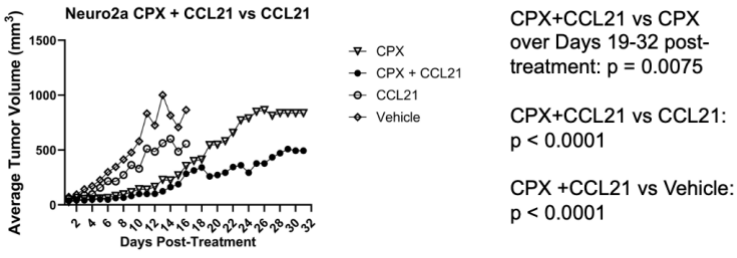

CCL21 therapy in conjunction with low dose cyclophosphamide (CPX) was superior to cyclophosphamide or CCL21 alone in controlling tumor growth in mice bearing neuroblastoma tumors. In addition, one mouse treated with both CCL21 therapy and low dose chemotherapy achieved complete tumor regression. Comparison of tumor volumes between dual treatment and CPX alone were conducted via Linear Mixed Model analysis. Comparisons of dual treatment vs. CCL21 or dual treatment vs. vehicle were conducted with unpaired t-test. (n=6 per group, reflective of one independent experiment)

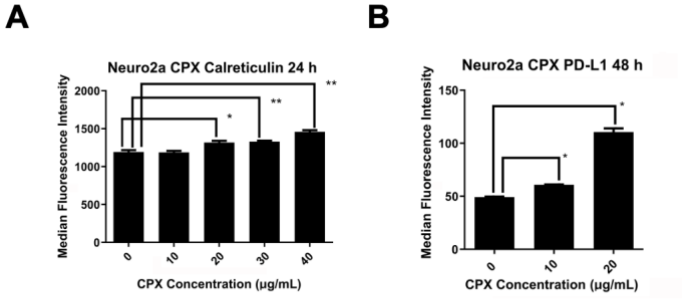

(A) Flow cytometry analysis demonstrated that low-dose cyclophosphamide (CPX) increases neuroblastoma cell expression of cell-surface calreticulin, a damage signal capable of stimulating anti-tumor immunity. (B) In addition, flow cytometry analysis showed that low-dose cyclophosphamide increases the expression of PD-L1, an inhibitory molecule known to inactivate T cells. * = $p < 0.05$ and ** = $p < 0.0.01$ Comparisons of MFI conducted by unpaired t-test (reflective of 3 independent experiments)

INVESTIGATING THE ROLE OF THE SAMD1 SAM DOMAIN IN ERYTHROPOIESIS

Samantha Gomez, Meg Schaefer, Kyle Hewitt (UNMC Omaha, NE)

Erythropoiesis is the process by which red blood cells (RBCs) are formed. Changes in the rate of erythropoiesis occur as a response to stressors – including anemias – and are controlled by intrinsic and extrinsic factors. Important intrinsic regulators include transcription factors (e.g. GATA2) that control proliferation, differentiation, and survival of RBC precursors. GATA2 mutations can cause several hematological diseases such as myelodysplastic syndrome, lymphomas, and anemia. Our lab discovered that a sterile alpha motif (SAM)-containing protein called SAMD1 controls expression of GATA2 in erythroid precursors, and lowering SAMD1 expression increases erythropoiesis. SAM proteins can self-polymerize, associate with other SAM-containing proteins, bind to non-SAM proteins, or bind to RNA and DNA, to perform diverse cell functions. Samd1 has been defined as a transcription factor that interacts with L3MBTL3/4, SFMBT1/2, and other components of a transcriptional repressor complex. While Samd1 is highly expressed in erythroid progenitors, regulates GATA2, and controls histone methylation patterns in differentiating cells, its role in erythropoiesis is not known. **I hypothesize SAMD1 erythroid transcriptional programs are coordinated in a SAM-domain dependent manner.** To evaluate SAMD1 function in erythropoiesis, we are conducting molecular, transcriptional, and functional assays in erythroid cells**.** We performed SAMD1 CUT&RUN sequencing in erythroid cells to identify SAMD1 occupancy sites on chromatin. We observed SAMD1 occupancy at both the promoter and enhancer regions of the GATA2 locus correlated with changes in H3K4 methylation status after SAMD1 knockout, suggesting SAMD1 directly regulates GATA2 expression in erythroid precursors. Utilizing truncation mutants of SAMD1, we will evaluate the role of the DNA-binding winged helix and SAM domains of SAMD1 on erythropoiesis and SAMD1-dependent transcriptional activity. We are using the immortalized but otherwise normal human erythroid precursor cell line HUDEP-2, which can be differentiated to mature erythrocytes. After genetic ablation and rescue of SAMD1 expression with inducible SAMD1, SAMD1-ΔSAM or SAMD1-ΔWH expression vectors, I will test my hypothesis by evaluating SAM-dependent chromatin occupancy (by CUT&RUN-sequencing), SAM-dependent expression changes (by RNA-seq), erythroid maturation (by flow cytometry), and morphological evaluation (by Wright-Giemsa staining). These experiments will provide valuable new information the precise molecular mechanisms of the Samd1-SAM domain. Understanding the role of SAMD1 in erythropoiesis (and perhaps more broadly in hematopoiesis) will shed light on both fundamental processes of RBC production and possible avenues of treatments.

LYSINE ACETYLATION IS ESSENTIAL FOR *B. BURGDORFERI'S* SURVIVAL UNDER STARVATION

E. Rose Grothaus, Meera M. Cao, Travis J. Bourret (Creighton University, Omaha, NE)

Background, Significance, Hypothesis: Lyme disease is the most common vector borne disease in North America and Europe, with an estimated 476,000 new cases yearly in the United States. Lyme disease is caused by the extra-cellular bacteria, *Borrelia burgdorferi*. This bacterium is transmitted to mammalian hosts by being fed on by the hard bodied tick vector, *Ixodes spp*. In *B. burgdorferi's* enzootic cycle it encounters diverse environmental challenges from the tick vector and the mammalian hosts, to survive this *B. burgdorferi* must adapt to rapidly changing host environments. These environment shifts include changes in temperature, pH, osmolarity, nutrient availability, and host-derived reactive oxygen species and reactive nitrogen species. The availability of nutrients is of particular note because the bacteria have to survive in the tick vector over the winter when the tick will go months without a blood meal. The widespread differences in the transcriptomes of *B. burgdorferi* residing in their mammalian and tick hosts are well documented. While transcriptional and translational changes have been studied, the role of post translation modifications (PTM) has not been investigated to understand their potential role in protein regulation as this bacterium navigates its diverse environments. In this work, we investigate the PTM, lysine acetylation's role in survival under low nutrient availability. Previous work determined that the acetyl donor for lysine acetylation in *B. burgdorferi* is acetyl-phosphate which is only present in the mevalonate pathway as *B. burgdorferi* lacks a TCA cycle. It has also been shown that the lysine acetylation of key glycolytic enzymes in *B. burgdorferi* lowers their enzymatic activity which could conserve energy when nutrient availability is lower. This led to our hypothesis that lysine acetylation aids in the survival of *B. burgdorferi* under nutrient limited conditions.

Experimental Design: To test this hypothesis, we determined the survival rate of the knockout of acetate kinase (*ackA)* A3B31 *B. burgdorferi* referred to as Δ*ackA* and of the knockout of phosphate acetyltransferase (*pta)* A3B31 *B. burgdorferi* referred to as Δ*pta* in Roswell Park Memorial Institute Medium (RPMI). The strain Δ*ackA* lacks *B. burgdorferi'*s only acetyl donor, acetyl phosphate, and Δ*pta* has an excess of it. RPMI is used to mimic the more limited nutrient availability found in the tick vector. The cultures were plated in pBSK (plating Barbour-Stoenner-Kelly) at 0hr and 48hr timepoints and colony forming units were then counted to compare survival rates to WT *B. burgdorferi*.

Results/Data: The results from the plating assay had Wt, Δ*pta* and Δ*ackA* similar levels at the 0hr time point with their respective cell densities calculated at 5.9×10^6, 1.3×10^7,3.4×10^6. After 48hr in the RPMI, Δ*ackA* had no colonies form while both Δ*pta* and wild type were able to survival with cell densities of $4.0 \times 10^4$and 8.3×10^3.

Conclusions: The results support our hypothesis that lysine acetylation aids in the survival o*f B. burgdorfer*i under nutrient limited conditions as after 48hr in RPMI the strain Δ*ackA,* which lacks the ability to undergo lysine acetylation, had no surviving spirochetes where both WT and Δ*pta,* which has excess of the acetyl donor, survived at similar levels.

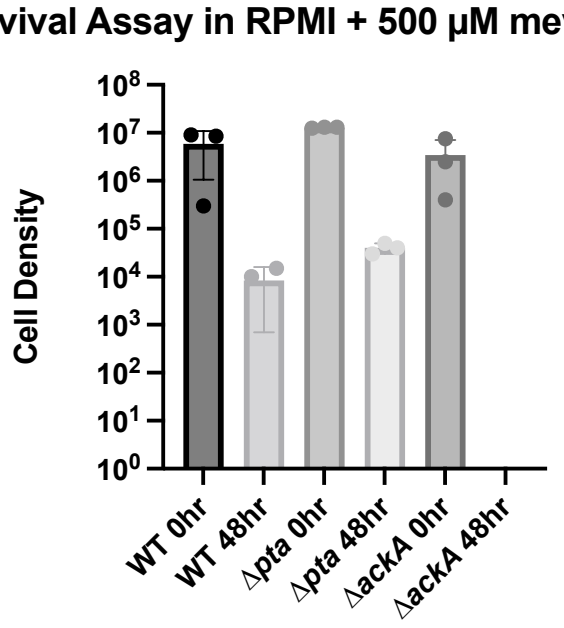

.

GOING NUCLEAR WITH LEVAMISOLE: ROLE OF DAF-12 IN MODULATING CHOLINERGIC TACHYPHYLAXIS

Shruti Gupta, Shannon Kennicutt, Jacob Wragge, Sudhanva Kashyap, Creighton University, Omaha, Nebraska

Helminth infections such as ascariasis, and lymphatic filariasis, caused by parasitic nematodes, **affect more than a billion people** in the tropical and sub-tropical countries. Ascariasis is a soil-transmitted helminth infection and primarily infects children in poor sanitation areas. Lymphatic filariases are a group of filarial nematode diseases transmitted by mosquitoes and cause gross inflammation of the lymphatic system. These infections are not life threatening but considered a societal burden as they impact education and workforce participation thereby leading to a continuous cycle of poverty.

Due to lack of effective vaccines, anthelmintic drugs are used to control these diseases. **Levamisole**, an old, classical anthelmintic used to treat ascariasis, reduces worm burden in the host by activating the **nicotinic acetylcholine receptors (nAChRs)** leading to an influx of calcium and causes nematode muscle paralysis. However, adult worms recover in the presence of the drug through an unknown mechanism called **cholinergic tachyphylaxis**. These worms persist in the body of the host and propagate the disease for many years and contribute to anthelmintic drug resistance. Therefore, understanding the mechanisms of worm recovery in the presence of levamisole is critical in the development of resistance-busting drugs.

In our study, we use both free-living nematode, *Caenorhabditis elegans* and parasitic nematode *Brugia malayi* as models to understand the molecular drivers of tachyphylaxis. In *B. malayi*, cholinergic tachyphylaxis was attributed to the **downregulation of *nra-2*** transcript. NRA-2 retains misfolded nAChRs in the endoplasmic reticulum. The reduction of NRA-2 in the presence of levamisole results in the **translocation of misfolded nAChRs to the membrane**. These receptors are insensitive to levamisole but their sensitivity to the endogenous ligand, acetylcholine, enables the worms to recover. Interestingly, **wild-type *C. elegans* do not recover** in high levamisole concentrations similar *to* male *B. malayi*. However, our results show that, in *C. elegans,* ***nra-2*** **mutants recover robustly** in lower concentrations of levamisole. Pharmacological intervention of the modulation of *nra-2* expression could prevent cholinergic tachyphylaxis. We hypothesize that the transcription factor that controls *nra-2* expression can be characterized as a novel anthelmintic target to prevent worm recovery. Sequence analysis of *B. malayi* and *C. elegans'* genomes reveal enrichment in **DAF-12 recognition sites in the promoter region of *nra-2*,** suggesting that DAF-12 could modulate the expression of *nra-2* in nematodes. We observe an upregulation of *daf-12* transcript in female *B. malayi* exposed to high concentrations of levamisole, suggesting a role for DAF-12 in cholinergic tachyphylaxis. In *C elegans*, ***daf-12*** **mutants recover in the presence of 300µM levamisole** suggesting *daf-12* activation could prevent worm recovery. Interestingly, *daf-12* and *nra-2* are expressed 56.31- and 12.5-fold higher in males compared to female *B. malayi*. Here we determine the relationship between *daf-12* and *nra-2* and their role in recovery in *C. elegans* and *B. malayi* and characterize **DAF-12 as a potent anthelmintic target to prevent levamisole recovery**.

TARGETED SEQUENCING FOR HEREDITARY CANCER RISK VARIANTS IN THE LYNCH MEMORIAL BIOBANK

Sun Young Guwn, Holly Stessman (Creighton University Omaha, NE)

Background and Significance: Breast, gynecologic, and colon cancers are one of the leading causes of cancer-related death among family members and are commonly genetically linked. Although many of these cancers are characterized with specific single-gene mutations, many individuals are likely unaware that they carry a risk allele without genetic testing, which is currently not recommended to the general public without specific indications, such as presenting with significant family history. Since hereditary cancer (HC) is determined retrospectively, after patients were diagnosed with cancer and received genetic testing as a result, the population that have these risk alleles are likely underestimated. In addition to the 20 genes identified to have HC risk with established medical management guidelines, including the BRCA1/2 genetic variants, preliminary research has demonstrated that there are additional genes without established medical management that may show relevance to HC risk, rated as “Variants of Unknown Significance (VUS).” By screening patients that come to clinics preemptively for high-risk HC genes and variants, we will be able to take prophylactic measures to decrease incidence rates of cancer diagnoses.

Hypothesis: We hypothesize there are more genetic variants that influence the development of cancer in affected individuals than the 20 confirmed genes currently listed in medical management guidelines. Additionally, we hypothesize the combination of certain variants and mutants in conjunction with each other may cause an additive effect in the individual, causing cancer to manifest differently than when an individual carries a single variant.

Experimental Design: Utilizing data from the Lynch Memorial Biobank, we are able to analyze the details of a specific variant including pathogenicity, associated gene, the exact nucleotide variant in the cDNA and subsequent amino acid variation and position in the protein. Additionally, we analyzed the formal clinical diagnoses made in individuals in family pedigrees, where some family branches demonstrated strong cancer correlation suggesting genetic influence. By comparing the pedigree data to the DNA sequencing data in the Biobank, we can draw conclusions from the effect of these variants and identify the effect of VUS and its role in influencing cancer diagnosis, especially as they track through multiple family members horizontally and vertically.

Data and Results: Among the 30 families analyzed in the Biobank, several families produced data that suggests certain VUS variants may have pathogenetic properties that have not previously been noted as significant. Family 1 demonstrates individuals with multiple variants display cancer diagnosis at earlier ages, suggesting a compounding effect of specific variants. A branch in Family 2 demonstrated a VUS variant in the CHEK2 gene that was always associated with a formal cancer diagnosis. Individuals in Family 4 with the BRCA1 legacy variant and another variant in another gene often reported cancer, suggesting the BRCA1 variant is increasingly pathogenic with additional variants in other genes. A male individual in Family 6 carried pathogenic variants in the BRCA1 and CHEK2 genes and also reported breast cancer, which suggests the additive effect of these two pathogenic variants could cause an increased risk of breast cancer in a population in which breast cancer is rare.

Conclusion: Analysis of several families in the Lynch Memorial Biobank demonstrated cancer diagnoses while the individual was only genetically confirmed to carry a VUS level variant, indicating a previously undocumented pathologic effect for individuals with this variant. By identifying previously undocumented variants in patients, we may positively impact HC prevention and management for patients with significant HC risk found upon screening.

CHROMOSOMALLY ENCODED RPOC_10XH, A NEW TOOL FOR INVESTIGATION OF THE CHLAMYDIAL TRANSCRIPTOME DURING STRESS

J. Cole Holderjano, Nathan D. Hatch, and Scot P. Ouellette (UNMC, Omaha, NE)

Background, Significance, and Hypothesis

Chlamydia trachomatis is an obligate intracellular bacterium, the leading cause of infectious blindness, and the most costly sexually transmitted non-viral infection. Many chlamydial infections have been linked to a chronic growth state, termed persistence, that is induced in cell culture by stressful conditions such as nutrient limitation. In evolving to intracellular dependence, Chlamydia has streamlined its genome size and content. The pathogen encodes three sigma factors (σ28, σ54, and σ66) and a handful of transcription factors. The exact roles of these transcription factors in the regulation of the chlamydial developmental cycle are not fully characterized. Currently, no comprehensive studies exist characterizing active transcriptional complexes in Chlamydia, and little is known regarding transcriptional start, pause, and stop sites, which may be important for transcriptional control of the developmental cycle. Furthermore, the limited genetic tools for Chlamydia have hampered the investigation and evaluation of alternate promoter sites and differential RNA polymerase (RNAP) occupancy. **We hypothesize that *Chlamydia trachomatis* utilizes these forms of gene regulation during response to nutritional and immunological stressors**.

Design and Evaluation

To test this hypothesis, we have generated a strain of Ctr L2 with a chromosomally encoded 10xHis-tagged RpoC, the β'-subunit of RNAP, using allelic exchange knock-in. This will allow for pulldown of the subunit via a His-targeting antibody, enabling ChIP-seq evaluation of the transcriptome.

Clones generated during the knock-in were evaluated for successful integration of both the modified RpoC and a penicillin resistance cassette. We have shown that the strain phenocopies wild-type Ctr L2 in developmental cycle progression, infectious progeny production, and response to tryptophan deprivation. Additionally, we have demonstrated that integration of the tagged RpoC does not impact the transcription of representative genes throughout development. Finally, we have successfully performed RpoC_10xH pulldown from this strain and eluted DNA fragments correctly sized for ChIP-sequencing (Figure 1).

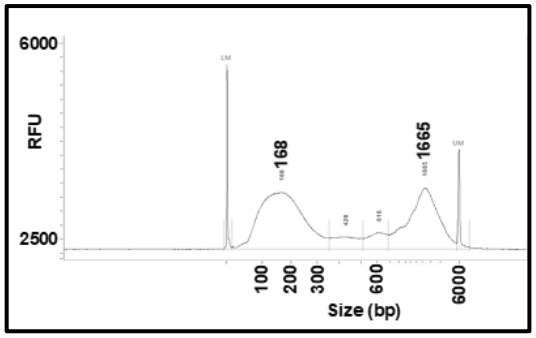

Figure 1: DNA fragment analysis from crosslinked, pulled down Ctr RpoC_10xHis

Future Directions

We will use this strain to perform RNA-seq and ChIP-seq with *Chlamydia* during tryptophan deprivation. We will evaluate changes in RNAP occupancy and transcription during normal growth and stress conditions. Ultimately, these data may directly identify alternative promoter sites and differential RNAP occupancy that impact control of the chlamydial transcriptome, allowing for a more complete understanding of how this organism persists despite immune-mediated stressors.

CK2α IS A NOVEL PHOSPHOINOSITIDE EFFECTOR IN DNA DAMAGE REPAIR

Gavril Ibaan[1], Suyong Choi[1]
1. University of Nebraska Medical Center, Omaha, NE

Background, Significance and Hypothesis: Phosphoinositides (PIs) are lipid secondary messengers critically involved in a plethora of membrane centric functions such as vesicular trafficking and cytoskeleton dynamics. PIs are generated by lipid kinases which themselves can be directly involved in signaling pathways by binding to proteins, this allows the kinase to generate PIs to specifically and efficiently bind and regulate an effector. Unlike the general belief, a significant fraction of PIs is found in non-membranous nuclear compartments; in particular we have previously demonstrated that levels of nuclear phosphatidylinositol 4,5-bisphosphate ($PI4,5P_2$) increase under DNA damage, however their function still remains largely enigmatic. Among the nuclear localizing lipid kinases, pools of $PI4,5P_2$ are generated by PIP4K2A and PIP4K2B using phosphatidylinositol 5-phosphate (PI5P) as a substrate, but $PI4,5P_2$ effectors directly regulated by PIP4K2A and PIP4K2B remain to be identified. To this end, we performed proteomic screens to reveal novel interactors of PIP4K2A and PIP4K2B. We found that the protein kinase CK2 catalytic subunits CK2α and CK2α' (encoded by CSNK2A1 and CSNK2A2, respectively) associate with PIP4K2A and PIP4K2B in a breast cancer cell line. The identification of PIP4K2A and PIP4K2B's novel interaction is intriguing as CK2α is reported to translocate into the nucleus and regulate a diverse set of nuclear pathways including DNA damage repair (DDR). Moreover, high levels of PIP4K2A, PIP4K2B and CSNK2A1 expression is associated with poor prognosis in breast cancer. Cancer cells are subject to large amounts of mutational burden and after the initiation stage the increased activation of DDR can improve cancer cell survival by preventing further damage. In this light, we hypothesize that PIP4K2A and PIP4K2B associate with CK2α and generate $PI4,5P_2$ which facilitates the phosphorylation of CK2α dependent DDR proteins and induces repair. Considering that CK2α is unbiasedly overexpressed in essentially all types of cancer the PIP4K2A/PIP4K2B-CK2α interaction provides a promising avenue for illuminating the role of nuclear PIs in cancer.

Experimental Design and Results: Identification of PIP4K2A/PIP4K2B interactions with CK2α in the proteomic screen was further validated via immunoprecipitation (IP). Endogenous CK2α was co-IPed with endogenous PIP4K2A/PIP4K2B in MDA-MB-231 breast cancer cell lines. Co-IP experiments after overexpression in HEK293T cells showed that comparatively more PIP4K2A interacts with CK2α compared to PIP4K2B. We next tested if PIP4K2A/PIP4K2B interactions with CK2α are direct by performing *in vitro* binding assays with recombinant proteins expressed in *E. coli*. Recombinant PIP4K2A was pulled down with CK2α, whereas no pulldown of PIP4K2B was observed, indicating that PIP4K2A but not PIP4K2B directly binds to CK2α. Interestingly, the addition of recombinant PIP4K2A in the PIP4K2B-CK2α *in vitro* binding assays rendered PIP4K2B association with CK2α. Considering the previous reports showing that PIP4K2A and PIP4K2B can form a heterodimer, this result suggests that CK2α forms a complex with a PIP4K2A-PIP4K2B heterodimer in cells. Protein-lipid overlay assays revealed that CK2α binds PI species including $PI4,5P_2$ with variable binding affinities. Our cell biological and biochemical assays further showed that the vast majority of CK2α interaction to PIP4K2A, PIP4K2B, and $PI4,5P_2$ occurs in the nucleus and, importantly, the interactions were increased by genotoxic stress by cisplatin. Functionally, PIP4K2A and PIP4K2B were required for phosphorylation of CK2α substrates involved in the DDR pathway such as XRCC1 in response to cisplatin treatment.

Conclusion: Our data supports the hypothesis that PIP4K2A and PIP4K2B modulate CK2α's ability to phosphorylate DDR proteins upon genotoxic stress. This study elucidates a previously unknown role of nuclear PIs in regulating DNA damage repair.

IDENTIFICATION AND VALIDATION OF NOVEL TARGETS FOR THE TREATMENT OF CUTANEOUS SQUAMOUS CELL CARCINOMA

Moynul Islam, Justin Rudd, Louise Monga, James A. Grunkemeyer, and Laura A. Hansen
Creighton University, Omaha, NE

Background: Cutaneous squamous cell carcinoma (cSCC) is a form of skin cancer which affects approximately 1.8 million people annually in the US and the number of patients diagnosed with cSCC is increasing each year. The orchestrated movement of proteins and RNA between the nucleus and cytoplasm is critical for cellular homeostasis. This essential shuttling process hinges upon specialized molecular players, namely Importins, Exportins and Transportins. The irregular functioning of any of these molecular transporters has the potential to disrupt the precise localization of cargo molecules (proteins or RNA), thereby impacting cellular health. Exportins, with their pivotal role in transporting a multitude of cargoes from the nucleus to the cytoplasm, have garnered considerable scientific interest in the context of tumor development. Notably, Exportin 1 (*XPO1*) is responsible for translocating approximately 400 cargoes including tumor suppressor proteins and growth regulators. *XPO1* expression is increased in multiple cancer types. Preliminary data from our lab shows that *XPO1* is also overexpressed in actinic keratosis (a pre-malignant lesion) and cutaneous squamous cell carcinoma (cSCC). Additionally, we found that Selinexor, an FDA approved Exportin 1 inhibitor, causes cellular toxicity in a panel of cSCC cell lines with IC_{50} ranging from 0.071 µM to 0.74 µM and increases apoptosis in these cell lines. However, the challenges of limited effectiveness, and the potential for toxicity to normal cells is a concern with Selinexor clinical use. This project aimed to identify and validate additional targets that could enhance the effectiveness of Selinexor in treating cSCC, and so allow for its use at a lower dose, by utilizing a genome-wide CRISPRi screening system.

Significance of Problem: Given the increasing incidence of cutaneous squamous cell carcinoma (cSCC) in the United States, it is important to identify highly effective chemotherapeutic options. Genome-wide CRISPRi screening holds the potential to uncover specific targets which can be used in combination with Selinexor to increase its effectiveness for cSCC treatment.

Hypothesis: Genome-wide CRISPRi screening in combination with Selinexor treatment will identify targets that increase the sensitivity of cSCC cells to Selinexor.

Experimental Design: Human cSCC SCC-13 dCas9-KRAB cells were developed for the genome-wide CRISPRi screen. SCC-13 dCas9-KRAB cells express dCas9-KRAB, a nuclease-deficient Cas9 enzyme fused to the KRAB transcriptional inhibitor (a domain of ZNF10). To perform genome-wide CRISPRi screen, SCC-13 dCas9-KRAB cells were transduced with lentivirus at 0.4 MOI (Multiplicity of Infection) which were packaged with Dolcetto Set A (Addgene #92385) genome-wide CRISPRi guide RNA library. The library contained 57,050 guides targeting 18,901 genes. After successful lentiviral transduction and Puromycin selection, 160 million cells were split into two groups. One group was treated with vehicle and the other group was treated with Selinexor at the IC_{15} for two weeks. Cells were sub-cultured every 3 days by plating 80 million cells per group. Genomic DNA was extracted, and PCR amplification of the guides was performed. Illumina sequencing of the PCR products was performed and the guide RNA abundance in Selinexor versus vehicle was analyzed by MAGeCK followed by gene set enrichment analysis of the depleted genes for identifying pathways which potentially increase sensitivity of cSCC to Selinexor. Commercially available inhibitors for selected target genes from the screen; including BIRC5, ALDOA, SRSF3 and NRF1; were used to treat SCC-13 cells in combination with Selinexor followed by Resazurin assay to determine cell viability.

Results: From the genome-wide CRISPRi screen with Selinexor, 293 target genes ($p < 0.05$ and $\log_2$foldchange < -0.58) were identified as increasing the sensitivity of the cSCC cells to Selinexor. These targets were significantly enriched in pathways of RNA processing and the cell cycle. YM155 (BIRC5 inhibitor), Aldometanib (ALDOA inhibitor), SFI003 (SRSF3 inhibitor), and WRR139 (NRF1 inhibitor) showed increased cell death when combined with Selinexor.

Conclusions: We have identified 293 targets through genome-wide CRISPRi screen that have the potential to increase the sensitivity of cSCC to Selinexor treatment. Several targets from the list have been validated through the use of inhibitors combined with Selinexor. Additional targets from the list will be tested to validate their sensitizing effect on cSCC. The identified and validated targets may have utility for combinatorial treatment in other cancers in addition to cSCC.

TRENDS IN EMPHYSEMA-RELATED MORTALITY IN THE UNITED STATES (1999-2022)

Amanda Karl, Alexandra Brown, Vikram Murugan, Taylor Billion, Abubakar Tauseef (Creighton University School of Medicine, Omaha, NE)

Background, Significance, Question: Pulmonary emphysema is considered a subtype of Chronic Obstructive Lung Disease (COPD). It is a progressive lung disease characterized by persistent respiratory symptoms that are a result of destruction to the alveoli wall and permanent enlargement of distal airspaces. It has been well-documented that emphysema is frequently the result of chronic exposure to toxins, most notably cigarette smoke which remains the most common cause of emphysema in the United States. In response to persistent exposure to cigarette smoke, inflammatory cells are recruited resulting in downstream effects that damage the alveoli and distal airways, including proteinase secretion, mucus hypersecretion, and large cytokine release. Despite initiatives made to create awareness about the dangers of smoking, and a nationwide reduction in cigarette smoking, it is worth noting that emphysema (COPD) is still the third leading cause of death in the United States and the fourth leading cause of death worldwide. Previous research has utilized CDC WONDER from 2004 to 2018 to demonstrate that chronic obstructive pulmonary disease (COPD) mortality has decreased among Americans. This study will expand on past research by looking at emphysema deaths in a wider time frame and in more recent years, from 1999 to 2022.

Experimental Design: This study utilized the Centers for Disease Control and Prevention Wide-Ranging Online Data for Epidemiologic Research (CDC WONDER) national database to investigate the trends in emphysema-related mortality in the United States. CDC WONDER provides a wide range of public health data including births, deaths, cancer diagnoses, vaccinations, and/or environmental exposures. Using this database, age-adjusted mortality rates per 100,000 people (AAMR), annual percentage change (APC), and average annual percentage change (AAPC) with 95% confidence intervals (CIs) were assessed. The Joinpoint Regression Program was used to determine mortality trends between 1999 and 2022 based on demographic and regional classifications. Data extracted for analysis in this study includes gender, race/ethnicity, age groups, regions, states, and urban/rural classification.

Results and Data: From 1999 to 2022, there were 526,545 deaths due to emphysema in the United States. Overall age-adjusted mortality rates (AAMR) in the United States decreased from 18.47 in 1999 to 7.75 in 2022, with an average annual percentage change (AAPC) of -3.698. From 1999 to 2022, emphysema caused 296,859 deaths in males and 229,686 in females in the United States. The AAMR decreased in females from 13.67 in 1999 to 5.96 in 2022. In males, the AAMR decreased from 25.95 in 1999 to 10.06 in 2022. White populations had the highest AAMR over this time period and the largest reduction in AAMR. Asian or Pacific Islander populations had the lowest AAMR consistently from 6.58 in 1999 to 2.53 in 2022. When comparing regional density and development, AAMRs were initially highest in urban areas compared to rural regions. Among studied age groups, 85+ years had the highest crude mortality rate of 123.11 in 1999.

Conclusions: The results of this study demonstrate that emphysema-related deaths in the United States decreased overall between 1999 and 2022, and this is likely a result of a greater emphasis on health education concerning the significant dangers of smoking and policy changes that made cigarettes less accessible and less affordable, as well as easier and more available access to resources and support networks for those who want to quit smoking. Of the demographic groups analyzed, mortality was highest in White populations, older adults, those living in urbanized areas, and males. These results could be attributed to the fact that it has been well-documented previously that White populations have an increased prevalence of smoking than other races. Older populations are more likely to see a decline in lung function and increases in other comorbidities than younger populations. Those living in urban areas are exposed to more air pollutants than those in rural areas. There continues to be little research into the gender differences that are seen with emphysema-related mortality rates. It is worth noting that these are extrapolations of mortality data, and warrant further research and a better understanding of a patient's comorbidities or risk factors for reliable conclusions to be made from the data. The aim of this study was to illuminate the trends that exist among various population factors. To work towards increasing health equity throughout the United States, it is imperative to consider these differences, along with resource allocation, in order to minimize the differences observed in mortality trends and improve healthcare outcomes among all population groups.

Epidemiology of Wrestling Injuries in Female Athletes at US Emergency Departments

Jasmeet Khera[1], Nikhil Furtado[1], Sai Geetika Guturu[1], Jacob Lin[1], Matthew Dilisio[1,2]
[1]Creighton University School of Medicine Omaha, NE
[2]OrthoNebraska Omaha, NE

Background, Significance and Hypothesis

Women's wrestling is one of the fastest-growing sports in the United States. The sport now has over 50,000 participants at just the high school level in 2023 versus just 804 in 1994 with 2023 being the year where women have their own officially established weight classes rather than having the same weight divisions as the men. Wrestling has one of the highest injury rates at 2.5 per 1000 athlete exposures, second only to football which was 4.36 per 1000 athlete exposures. Unlike other sports, wrestling male and female wrestlers practice with each other and compete against one another from the youth level up to the high school level. Guidelines and regulations surrounding their participation are different with men being allowed to be at a minimum of 7% body fat and women 12% according to NWCA guidelines. Regulations have been put in place to minimize injuries as excessive weight-cutting has been shown to increase the risk of injury. Youth wrestling does not have the same rules and regulations as the high school level with many different community organizers running events and many private clubs operating within communities. Wrestling injuries in female athletes is an understudied topic. The aim of this study is to characterize the injuries that occur in female wrestlers aged 5–18-year-old who presented to United states (US) emergency departments (ED) from 2014-2023 and compare patterns between youth and adolescent wrestlers. Do the injury patterns and mechanisms significantly differ between youth (5-11) and adolescent (12-18) and can these differences inform injury prevention strategies for these populations.

Experimental Design

A retrospective analysis was performed using data from the National Electronic Injury Surveillance System (NEISS). Female patients aged 5-18 presenting to the ED due to wrestling-related injuries were included. Patient demographics, injury location, and diagnosis were analyzed. Chi-squared tests compared injury distributions between age groups.

Results

An estimated 28,824 female wrestlers (841 NEISS cases) presented to U.S. EDs during the study period. The most frequently injured body parts were the head (16.5%), shoulder (14.0%), knee (11.1%), and elbow (10.7%). Strains/sprains were the most common injuries in both youth (27.9%) and adolescents (30.3%). Fractures were significantly more common among youth wrestlers (23.1%) compared to adolescents (13.6%, $p < 0.05$). The distribution of injured body parts was also significantly different between groups ($p < 0.05$). In youth wrestlers, the most common injury sites were the head (11.5%, 95% CI 20.0-57.7%), wrist (10.6%, 95% CI 9.85-47.4%), and elbow (9.6%, 95% CI 16.3-56.6%). For adolescents, the head (17.2%, 95% CI 24.9–34.9%), shoulder (14.9%, 95% CI 31.4–43.5%), and knee (11.7%, 95% CI 27.7–41.0%) were most frequently injured. Overall, more than 60% of injuries occurred above the waist in both groups.

Conclusion

Adolescent female wrestlers experienced more injuries compared to youth wrestlers, with most injuries occurring above the waist. Factors such as increased mat time, hormonal changes, and higher practice intensity may contribute to this disparity. Injury prevention strategies are recommended, including adequate mat spacing and rule enforcement during practices and increased recruitment into the sport. Further research is needed to identify mechanisms and specific techniques linked to higher injury risks to enhance safety in female wrestling.

COMPARISON OF ACUTE VERSUS CONVERSION TOTAL HIP ARTHROPLASTY IN FEMORAL NECK FRACTURES

Andrew Minchow, Grace Kugler, Erin Stockwell, John Rosenberg, Christopher Deans (UNMC, Omaha, NE)

Background, Significance, and Hypothesis:
More than 150,000 geriatric femoral neck fractures (FNFs) occur annually in the United States, costing $12 billion. FNFs are classified by the Garden classification; types 1 and 2 are considered nondisplaced and often treated with surgical fixation, while types 3 and 4 are considered displaced and often treated with arthroplasty. Rates of conversion to arthroplasty after fixation of a femoral neck fracture are reported from 10-30%. Both acute total hip arthroplasty (aTHA) for the treatment of femoral neck fracture (FNF) and conversion THA (cTHA) after prior hip surgery have demonstrated increased complications compared to primary elective THA, though studies directly comparing aTHA for FNFs versus cTHA after fixation of FNFs are sparse. The purpose of this study was to compare clinical outcomes between FNFs in patients ≥50 years of age who underwent aTHA versus those who underwent initial closed reduction percutaneous pinning (CRPP) with subsequent cTHA. We hypothesized that there would be no significant difference in clinical outcomes of aTHA as compared to cTHA for FNFs.

Experimental Design:
This multi-center retrospective review examined the records of all patients ≥50 years of age who underwent an aTHA or initial CRPP with subsequent cTHA for the management of FNF at two level 1 and one level 2 academic medical centers between 2012 and 2023. Patient, injury, fracture, surgery, and outcome variables were recorded. Key clinical outcomes compared between aTHA and cTHA cohorts included operative time, estimated blood loss, length of admission (LOA), as well as intraoperative or postoperative fracture, instability, revision, infection, pulmonary or cardiac events, and mortality. Patient demographic and clinical characteristic data were described by descriptive statistics. Fisher's exact test assessed the association of clinical characteristics with surgical approach (aTHA vs. cTHA). Independent sample t-tests were performed to compare patient characteristics and key clinical outcomes between the surgical approaches. Results with a p-value > 0.05 were considered statistically significant.

Results:
Final statistical analysis included 466 patients, 421 of whom underwent aTHA and 45 of whom underwent cTHA. There were no significant differences in patient age, body mass index, or past medical and surgical history between the cohorts ($p>0.05$). Patients who underwent cTHA were significantly more likely to have had a Garden 1 or 2 fracture, while patients who underwent aTHA were significantly more likely to have had a Garden 3 or 4 fracture ($p<0.0001$). During their initial course of management with CRPP, the cTHA cohort had a shorter first length of hospital admission and operative time as compared to the aTHA cohort. However, conversion required longer operative time and greater total admission days than patients who underwent aTHA. Patients who underwent cTHA were significantly more likely to require THA revision for instability as compared to the aTHA cohort ($p=0.0279$). No statistically significant differences were noted between the aTHA and cTHA cohorts across all other clinical outcomes. However, patients who underwent cTHA were insignificantly more likely to experience an intraoperative FNF, intraoperative cardiac or pulmonary event, postoperative implant instability, and postoperative venous thromboembolism than their aTHA counterparts ($p>0.05$).

Conclusion: In patients ≥50 years who sustain FNFs, the clinical outcomes of aTHA as compared to cTHA largely do not significantly differ. However, patients undergoing cTHA experienced higher rates of THA revision as well as longer operative time at time of arthroplasty and greater cumulative days of hospital admission. Additional studies with larger cTHA sample sizes are warranted to assess whether the benefits of FNF management with CRPP, such as reduced operative time and shorter LOA, are offset by the negative clinical outcomes brought about by a future cTHA.

Title: OVERALL SURVIVAL RATE AND DISPARITIES IN PATIENTS WITH ANAPLASTIC ASTROCYTOMA CONCERNING SOCIOECONOMIC FACTORS AND TREATMENT(S): A NATIONAL CANCER DATABASE (NCDB) ANALYSIS

Authors: Nigel Lang, Kevin Choi, Elijah Torbenson, Peter T. Silberstein, John Paul Braun (Creighton University School of Medicine Omaha, NE)

Background, Significance, Problem: Gliomas are the most frequently diagnosed form of brain tumors with high rates of malignancy and mortality. High-grade gliomas represent the very aggressive, malignant forms and may be characterized by an anaplastic morphology including anaplastic astrocytoma. Previously reported survival rate in patients is approximately 21.5 months. This tumor most commonly occurs in children between 5-9 years old and adults between 30-50 years old. A key motivation for this study is to improve knowledge and future care in high-grade gliomas by analyzing and comparing patient socioeconomic factors, treatments, and survival outcomes with anaplastic astrocytoma.

This study aims to determine if the overall survival rate varies disproportionately in patients based on socioeconomic factors (race, income, urban/rural location, facility type) and treatment modalities (observation, surgical resection, radiation, and chemotherapy).

Experimental Design: The National Cancer Database (NCDB) was utilized to identify patients diagnosed with anaplastic astrocytoma using the histology code 9401 from the ICD-O-3.2. Kaplan-Meier, Chi-Square tests, and multivariate Cox regression were performed. The data was analyzed using SPSS version 29 and statistical significance was set to $\alpha = 0.05$.

Results/Data: In this study, 7,063 patients diagnosed with anaplastic astrocytoma were analyzed. The overall mean survival time observed was 46 months. Patients with the shortest mean survival time of 14.8 months received radiation only, whereas the longest mean survival time of 64.5 months received the triple combination therapy. Patients had a mean age of 50 years old and were more likely to be female, have Medicaid, and a lower Charlson-Deyo Comorbidity score. Socioeconomic factors including urban versus rural location, primary payor, and Charlson-Deyo Comorbidity score were all associated with significantly worse survival odds ($p<0.05$). Patient race, income, and the facility type were not significant. The two most common treatment protocols were chemotherapy, radiation, and surgery (54.9%) or chemotherapy and radiation alone (20.5%). Further, multivariate Cox regression suggested that patients treated with this combination or both chemotherapy and surgery had significantly greater odds of survival compared to radiation alone ($p<0.001$).

Conclusions: This study demonstrated that patients with anaplastic astrocytoma treated with triple combination therapy had significantly greater odds of survival compared to radiation alone and had the longest mean survival time. Additionally, several disparities based on socioeconomic factors were found. These findings are suggestive of the need to reduce disparities and treat with certain modality combinations to improve survival rates in these patients.

TRENDS IN MYELOID-RELATED MORTALITY IN THE U.S.

Jenna Lehn, Hannah Fleming, Taylor Billion, Abubakar Tauseef (Creighton University School of Medicine, Omaha, NE)

Background, Significance, Hypothesis: Myeloid Leukemias (ML) are neoplastic disorders that cause the production of abnormal myeloid blood cells and irregular hematopoiesis. There is a lack of literature analyzing ML across multiple cancer types as opposed to individual cancers. This study sought to investigate trends in ML mortality from 1999-2022 and to identify demographic disparities by calculating age-adjusted mortality rates (AAMR) and average annual percent change (AAPC).

Experimental Design: ML mortality was analyzed from 1999-2022 in the U.S. using the CDC WONDER database. AAMRs were calculated per 100,000 people and stratified by region, state, urban/rural residence, gender, and race. The AAPC trends for the respective stratification were computed with the National Cancer Institute (NCI)'s Joinpoint Regression Program (Joinpoint V 4.9.0.0, NCI) with log-linear regression models.

Data/Results: From 1999 to 2022, there were 299,221 deaths due to myeloid leukemia in the United States. Each census region apart from the Midwest had a non-significant downtrend in mortality rate from 1999-2022, while the Midwest had a non-significant uptrend. States with an AAMR greater than the 90th percentile included Iowa, Kansas, Minnesota, North Dakota, and South Dakota. Conversely, states with an AAMR less than the 10th percentile included Connecticut, Hawaii, Nevada, New Mexico, and Wyoming. Across populated regions, AAMRs were persistently higher in rural areas as compared to small, medium, and large urban centers. Males consistently had the highest AAMR across each census region, and the Midwest had the highest AAMR for both males and females. The White race consistently had the highest AAMR across each region, and Asian or Pacific Islanders and Hispanic or Latinos had the lowest AAMR.

Conclusions: Myeloid Leukemia-related mortality between 1999–2007 did significantly decrease in the United States, but had a non-significant increase from 2007-2022, despite the creation of new treatments. The identifiers associated with the highest ML AAMR from this study were male sex, White race, and residence in rural areas of the Midwest, most notably in Iowa, Kansas, Minnesota, and the Dakotas. For Midwesterners, AAMR has not improved over time. Further research is needed to address Myeloid Leukemia-related mortalities across demographic and geographical disparities.

ADIPOCYTE SECRETOME IS ALTERED BY RADIATION, INDUCING PROSTATE CANCER MIGRATION

Kia Liermann-Wooldrik[1], Elizabeth Kosmacek[1], Dr. Rebecca Oberly-Deegan[1]
1. University of Nebraska Medical Center, Omaha, NE

Background

Prostate cancer is one of the most diagnosed cancers in the male population. While the overall 5-year survival rate is 97%, 20-30% of prostate cancer patients will experience signs of recurrence in their lifetime. One of the main risk factors associated with prostate cancer is obesity, or excess adipose tissue. Radiotherapy is a vital component of the treatment of many types of cancer, especially those in the pelvic region, such as prostate cancer.

Significance

Common radiotherapy treatments do not spare adipose tissue found in the abdominal region and, thus, are exposed to radiation. Understanding how radiation can alter adipose tissue, specifically in the context of cancer, could explain how and why metastasis and recurrence occur.

Hypothesis

We hypothesize that the secretome of adipose tissue is altered by radiation, triggering prostate cancer progression.

Experimental Design

In vitro studies designed to evaluate the impact of irradiated adipocytes on prostate cancer cells have been conducted using a transwell system. In the bottom well, 3T3-L1 cells were chemically differentiated into mature adipocytes and then subjected to 3 Gy of radiation for 3 consecutive days, or SHAM irradiated, before PC3, C42B, and LNCaP prostate cancer cells were seeded into a migration chamber above the adipocytes. The prostate cancer cells were allowed to migrate through the chamber towards the adipocytes for 48 hours and were collected, counted, and maintained in culture for further analysis of pro-tumorigenic qualities. The 3T3 adipocytes, following co-culturing, were assayed for metabolic alterations and oxidative damage. Adipocytes were treated with antioxidants, vitamin E and the novel BMX-001, as well as various pharmacological lipase inhibitors to block radiation-induced free fatty acid release.

In vivo, C57BL/6 mice received 7.5 Gy of radiation to their inguinal fat pads using a Small Animal Radiation Research Platform (SARRP) for 5 consecutive days. A month later, RFP-expressing RM1 prostate cancer cells were injected orthotopically. Tumor burden was assessed using IVIS imaging, measuring primary, and enumerating metastatic tumors. Using immunofluorescence, oxidative damage in the fat pads of irradiated mice was assayed.

Results

In vitro, co-culturing of prostate cancer cells with irradiated adipocytes (3T3-L1 cells) promotes a significant 2- to 3- fold increase in migration compared to co-cultured with unirradiated 3T3 cells, when validated across three different prostate cancer cell lines. The prostate cancer cells co-cultured with the irradiated adipocytes have a significant increase in intracellular lipid content ($p=0.0216$, 0.0045 observed in two different cell lines) when compared to the parental cells and pronounced morphological changes associated with an epithelial-to-mesenchymal transition. We determined that the adipocytes have increased lipase activity ($p=0.0120$) in both a time and radiation-dependent manner, allowing the prostate cancer cells to take up free fatty acids from the adipocytes. This was verified by the presence of Bodipy lipid staining in the prostate cancer cells following co-culturing with Bodipy-stained adipocytes. By treating adipocytes with antioxidants or lipase inhibitors, the radiation-enhanced lipase activity is decreased and prostate cancer migration halted.

In vivo, when fat pads are irradiated prior to orthotopic injection with prostate cancer cells, there is a 4-fold increase in tumor burden and number of metastases per mouse but no difference in the size of the primary tumor. Further analysis of the fat pads revealed that irradiated adipose tissue has a significant 2-fold or 3-fold increase in lipid peroxidation and DNA oxidative damage, respectively, compared to unirradiated adipose tissue. Irradiated adipocytes also exhibit an increased immune cell infiltration and secretion of lipids, as well as a 4-fold decrease in fat cell area when compared to unirradiated adipocytes.

Conclusions

Given this data, we postulate that radiation alters the secretome of adipocytes by inducing oxidative damage to the cells, increasing the amount of released free fatty acids. These free fatty acids are then taken up by prostate cancer cells causing migration and metastasis.

EFFECT OF ZINC SUPPLEMENTATION ON GROWTH/DEVELOPMENT IN INFANTS WITH BRONCHOPULMONARY DYSPLASIA

Presenter Naomi Lin (Creighton University School of Medicine, Omaha, Nebraska), Elizabeth Lyden (University of Nebraska Medical Center), Courtney Haney, Eric S. Peeples (Children's Nebraska)

Background, Significance: Over 10% of infants are born prematurely, often due to spontaneous causes or pregnancy complications like infections, diabetes, or hypertension. Among preterm infants, bronchopulmonary dysplasia (BPD) significantly affects growth and overall health, causing challenges such as learning delays, infections, speech and vision problems, and feeding difficulties. Growth limitations in this population may be linked to zinc deficiency, as the zinc needs and metabolism of infants with BPD are poorly understood. Studies suggest zinc supplementation can reduce mortality and improve growth, such as linear growth and weight, but few have focused on high-risk infants with BPD or assessed head circumference, a vital marker of brain growth and neurodevelopment. This study explored the associations between zinc supplementation and growth outcomes in infants with BPD.

Hypothesis: Zinc supplementation administered to preterm infants with BPD benefits the growth (head circumference/length/weight) during supplementation relative to growth trajectories immediately before and after supplementation.

Experimental Design: This retrospective case-control study investigated the impact of zinc supplementation on infants with bronchopulmonary dysplasia (BPD) in the Children's Nebraska newborn intensive care unit (NICU). Infants were excluded if they received only partial zinc supplementation (i.e. not a full 6 weeks) or if they did not survive to discharge. Growth trajectories were analyzed over three periods: the 3 weeks immediately prior to supplementation, the first (if they were treated for longer than 6 weeks) 6 weeks during supplementation, and the first 3 weeks post-supplementation. A linear mixed model was used with a random effect for patients and a fixed effect for time period, along with pairwise comparisons adjusted using Tukey's method to evaluate differences in weight, length, and head circumference across the pre-, during-, and post-supplementation phases.

Data and Results: Zinc supplementation significantly improved linear growth during the treatment period compared to both pre- and post-supplementation phases (Fig. 1). Length trajectory returned to baseline after supplementation ended. There were no significant changes in weight or head circumference growth across the study periods.

Conclusion: Zinc supplementation demonstrated a positive impact on linear growth during treatment, but this effect was not sustained after treatment cessation. Furthermore, zinc did not enhance weight gain or head circumference growth. These findings suggest the need for further investigation into whether the standard zinc supplementation dose, commonly used in other studies, is sufficient for BPD patients or if a higher dose may be required to optimize growth outcomes.

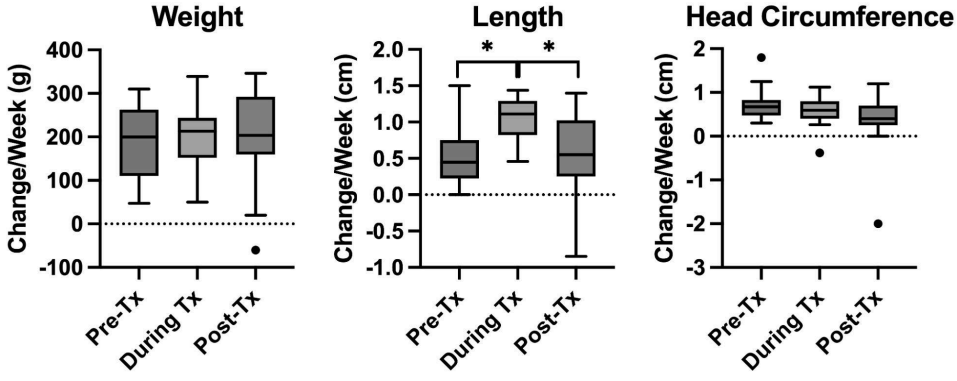

Figure 1. Changes in weight, length, and head circumference before, during, and after zinc supplementation. Line shows median and whiskers at Tukey limits, with outliers shown, *p<0.001

START-SITE ACCURACY COMPARISON BY APPROACH FOR TIBIAL SHAFT FRACTURES

Stevin Lu, Lukas Foster, Brett Ewing, Milton Little, Charles Moon, John Garlich, Geoffrey Marecek, Mark Vrahas, Carol Lin
Creighton University School of Medicine; Omana, NE

Background, Significance, Hypothesis: Tibial shaft fractures are a common type of lower extremity injury, with an incidence of 16.9 cases per 100,000 people annually. The preferred treatment for tibial shaft fractures is intramedullary nailing (IMN) due to its ability to provide stable fixation and promote early weight-bearing. Both suprapatellar and lateral parapatellar approaches for tibial IMN have been described. This study aims to evaluate differences in start-site accuracy for IMN fixation between the suprapatellar and lateral parapatellar approaches in tibial shaft fractures. We hypothesize that the suprapatellar approach will be more accurate as this approach is considered to provide more in-line access to the tibial canal.

Experimental Design: A retrospective study at a single Level I Trauma Center was performed between 2016-2023. Patients with tibial shaft fractures undergoing IMN fixation using either a suprapatellar or lateral parapatellar approach were included. Radiographic measurements were determined using AP and lateral fluoroscopic images, including displacement and angulation from the ideal start site position. Postoperative PROMIS scores and knee pain were collected at different time points: 3-months, 6-months, 12-months, and >12 months. In evaluating for differences in PROMIS (Physical Function, Depression, Pain) scores, patients were separated in 2 groups: within ±1 standard deviation (SD) or >±1 SD of AP and lateral measurement and angulation. Mann-Whitney U tests, mixed linear models, and chi-square tests were used to assess for statistical significance.

Data and Results: 248 patients met the inclusion criteria: 90 patients in the lateral parapatellar group and 158 patients in the suprapatellar group. The suprapatellar approach resulted in statistically closer guidewire positions to the ideal start site in AP (1.4 ± 0.8mm versus 1.7 ± 0.9mm) and lateral (1.3 ± 0.6mm versus 1.5 ± 0.8mm) fluoroscopic views ($p = 0.017$ and $p = 0.044$, respectively). The suprapatellar start site group also had less deviation from the optimal entry angle compared to the lateral parapatellar group in both AP (2.3° ± 1.4 versus 3.7° ± 2.1) and lateral (8.0° ± 4.8 versus 9.0° ± 4.6) fluoroscopic views ($p<0.01$ and $p = 0.036$, respectively). When controlling for age and BMI, AP measurement, AP angle, and lateral measurement using the suprapatellar start site remained statistically closer to the ideal start site ($p<0.05$). There were no significant differences in hospital length of stay, operation time and reoperation rates between the suprapatellar and lateral parapatellar groups ($p > 0.05$). Additionally, 116 of the 248 patients (44 in lateral parapatellar and 72 in suprapatellar) had data to evaluate for differences in PROMIS scores. No significant differences in PROMIS scores between patients within ±1 SD and those >±1 SD in AP and lateral measurement and angulation were seen at any time point ($p>0.05$).

Conclusion: This study suggests the suprapatellar approach may be a more accurate than the lateral parapatellar approach in obtaining an optimal start site for tibial IMN fixation, though this may not affect ultimate clinical outcome. Future research can explore differences in rates of misalignment after fixation between the two approaches that could potentially affect bone healing, deformity, and clinical outcomes.

ELEVATED INFLAMMATION IN PEOPLE WITH HIV IS ASSOCIATED WITH ABERRANT NEURAL OSCILLATIONS SERVING SELECTIVE ATTENTION

Kellen M. McDonald[1,2], Jake J. Son[1,3], Rachel K. Spooner[1], Mikki Schantell[1], Nathan M. Petro[1], Ryan Glesinger[1], Hannah J. Okelberry[1], Jason A. John[1], Matthew C. Zimmerman[4], Tony W. Wilson[1,2,3]

[1]Institute for Human Neuroscience, Boys Town National Research Hospital, Boys Town, NE
[2]Department of Pharmacology and Neuroscience, Creighton University, Omaha, NE
[3]College of Medicine, University of Nebraska Medical Center (UNMC), Omaha, NE
[4]Department of Cellular and Integrative Physiology, UNMC, Omaha, NE

Background: Medical advances have greatly improved the quality of life and extended the longevity of people with HIV (PWH). However, many PWH still develop neurocognitive deficits even in the presence of effective viral suppression, which can greatly impact their ability to perform daily activities. Deficits in selective attention are especially common and these have been linked to increased concentrations of neuroinflammatory markers and aberrant neuronal activity in primary sensory and higher-order cortical regions. A key component of selective attention is the ability to allocate attentional resources to relevant cues and inhibit irrelevant information. Previous investigations of selective attention with magnetoencephalography (MEG) have shown neural oscillatory activity in the frontoparietal network, particularly in the theta and alpha frequency ranges. However, it is unclear how elevated inflammation may impact this network among PWH and ultimately degrade selective attention function.

Hypothesis: Neuroinflammatory indices will be higher in PWH and differentially scale with frontoparietal neural activity during a Simon selective attention task compared to control participants.

Experimental Design: After excluding three participants for poor task performance, our sample consisted of 77 healthy controls and 70 PWH, with all PWH receiving antiretroviral therapy and confirmed to be virally suppressed. Whole blood was collected from all participants and plasma samples were subjected to an electrochemiluminescence-based multiplex immunoassay. Plasma concentrations of key biomarkers of neuroinflammation (i.e., TNF- α, CRP, and IP-10) were combined into one neuroinflammation index score per person via principal component analysis. In addition, participants completed a Simon task for assessing selective attention during MEG, which measures brain function by quantifying the magnetic fields that naturally emanate from active neuronal populations, providing spatially and temporally precise functional maps. For the Simon task, participants are shown three digits on the screen and identify via button press the digit that is different from the others shown, responding to the digit's numerical identity (i.e., 1, 2, or 3) and not its spatial location. The Simon effect is measured by subtracting the neutral condition, in which the numerical identity and spatial location match (e.g., 0 0 3), from the spatial interference condition, in which the identity and location do not match (e.g., 0 3 0).

Results: PWH had significantly lower accuracy on the task and elevated neuroinflammation index scores compared to controls. Simon interference maps were created by subtracting neuronal activity during the neutral condition from activity during the Simon interference condition. Whole-brain correlations using the interference maps were performed to examine the relationships between neural oscillatory activity ($p < .005$, corrected) during the task and neuroinflammation separately per group, and then these maps were compared using Fisher *r*-to-*z* transformation. In the theta frequency range (4-8 Hz), stronger responses in the dorsolateral prefrontal and premotor cortices (i.e., frontoparietal network) were associated with increased neuroinflammation index scores among PWH, whereas the opposite relationships were observed in the control group (dorsolateral prefrontal: $z = -4.21$, $p < .001$; premotor: $z = -3.51$, $p < .001$). Conversely, weaker alpha oscillations (8-14 Hz) in somatosensory and association cortices were significantly correlated with elevated index scores among PWH, while stronger alpha oscillations in the somatosensory cortex were correlated with decreased index scores among control participants (somatosensory: $z = -3.05$, $p = .002$; association: $z = -3.67$, $p < .001$).

Conclusions: Despite effective viral suppression, PWH exhibit greater concentrations of neuroinflammatory markers compared to healthy controls. Furthermore, greater inflammation among PWH was related to altered theta activity in regions of the frontoparietal network and abnormal alpha in regions necessary for sensory processing. It is possible that the altered relationships between oscillatory activity and neuroinflammation among PWH are indicative of future neurocognitive dysfunction. Interventions that target elevated neuroinflammation caused by HIV may mitigate HIV-associated cognitive decline.

INVESTIGATING MALIGNANT POTENTIAL OF VUS THROUGH GENEALOGICAL SURVEY OF CANCER INCIDENCE

Patrick McMonagle, Holly A. Feser Stessman (CUSOM Omaha, NE)

Background, Significance, Hypothesis: Lynch syndrome (LS) links colorectal, endometrial, ovarian, breast, prostate, and other commonly occurring cancers through mutations in MLH1, MSH2, MSH6, and PMS2 mismatch repair genes. In addition to these known mutations, thousands of variants of unknown significance (VUSs) are observed in the genomes of LS patients. While the impacts of VUSs are not fully understood, some may play a role in potentiation of malignancy. With LS affecting 1 in 279 people, identifying additional pathogenic mutations offers great promise for cancer screening and treatment. With greater knowledge of genes implicated in LS, more comprehensive genetic counseling may be offered to improve cancer screening for genetic carriers. In addition to presenting alongside individuals with known malignant variants, these VUSs will be present in individuals who developed cancers but did not have known pathogenic variants. Association of these VUSs with heritable cancers will help inform genetic testing for family members of patients with LS.

Experimental Design: Using next-generation sequencing (NGS) of samples from the more than 800 families with confirmed LS diagnoses, we identified the individuals with VUSs in each family to determine heritability patterns, genetic penetrance, and pathogenicity. Using Sanger sequencing, we confirmed the presence of the mutation in affected family members. Finally, pedigree analysis was used to compare genetic variants with observed pathogenicity. Examining the prevalence of cancer among family members carrying a deleterious gene permitted the estimation of impact and penetrance.

Data and Results: Review of genetic variation in the samples revealed VUSs present across generations. One such example could be found in family A, whose members expressed both known pathogenic and unknown mutations. While many of the pathogenic family members possessed the MHL1 gene, individual A-1 did not. Of the variants detected in individual 1, both PMS2 and NF1 were VUSs. Unlike in the previous family, sequencing of family B revealed no confirmed pathogenic variants, despite several members with phenotypic LS. Individual B-1 was confirmed to not carry an MLH1 variant, but she did have a VUS of the APC gene. B-1, her sister B-2, and her mother B-3 all presented with cancer diagnoses, and additional validations of the B-3's sample is pending. B-1's cousin, B-5, possessed a VUS of the PMS2 gene. While a lower percentage of her first-degree relatives reported cancers, both her parents and all her siblings provided tissue samples that allow future validations and cosegregation analysis to identify distinctions between symptomatic and asymptomatic individuals.

Conclusion: Genetic assessment of families with confirmed LS revealed individual variation and increases in the frequency of cancer even in family members without mutations in the genes that constitute LS. The presence of VUSs in other genes related to cell cycle regulation increased the risk of hereditary cancers, though these variants have differed in penetrance. The variants observed in family A were in genes with cancer associations which correlated with the pathologies observed. PMS2—a gene coding for a mismatch repair protein—and NF1—a tumor suppressor gene involved in several cell signaling pathways—may both have contributed to member A-1 receiving a diagnosis of ovarian cancer at age 33. In family B, variants in APC—a tumor suppressor gene regulating Wnt signaling—aligned with the pathology seen in family members. An APC gene mutation would correlate with the small bowel, colorectal, stomach, liver and breast cancers observed. While APC mutations are observed in familial adenomatous polyposis (FAP), family B members received diagnoses no earlier than 43 years of age, later than would be expected in FAP. In the family B relatives with the PMS2 variant, the observed colorectal and breast cancers would be expected. Further research should examine the associations of the variants present in each family, particularly to determine if their pathogenic effects are synergistic in individuals with multiple mutations.

RETROSPECTIVE REVIEW OF GESTATIONAL AGE INFLUENCE ON EXCLUSIVE BREASTFEEDING AT LAKESIDE AND BERGAN NEWBORN NURSERY

Eric Nguyen, Terence L. Zach (Creighton University School of Medicine, Omaha, NE)

Background, Significance, Hypothesis: The World Health Organization (WHO) and the American Academy of Pediatrics (AAP) recommend that mothers exclusively breastfeed their babies during the first six months of life. Breastmilk provides essential nutrients and non-nutritive components critical for babies' health and development. Breastfeeding also offers significant health benefits for mothers, including promoting postpartum weight loss, reducing stress, and aiding uterine involution. Common Spirit Health (CSH) aims for 65% of term babies to receive exclusive breastfeeding (EBF) in the newborn nursery. Previous research has investigated factors influencing EBF and developed methodologies to improve its rates. At Bergan Hospital, specifically, a prior study showed that gestational age influences EBF. This present study compares EBF rates by gestational age between Bergan and Lakeside hospitals relative to CSH's goals. By examining EBF rates across gestational ages, the study seeks to identify trends in EBF, creating baseline knowledge for future improvement in breastfeeding practices in hospital settings. EBF improvement will be critical in providing better health outcomes for both newborn babies and mothers. EBF will also play an important role in nourishing baby-mother early relationships through frequent skin-to-skin contact.

Experimental Design: A retrospective study was conducted, reviewing data from approximately 2000 medical charts of neonates at the newborn nursery at Bergan and Lakeside Hospital. The data collection period spanned from October 2023 to March 2024. Key data points included gestational age and mode of feeding (EBF or formula). EBF is defined as the infant only receiving the mother's breastmilk or the donor's breastmilk. If the infant receives any formula during hospitalization, they will no longer qualify for EBF.

Data and Results: At Bergan Hospital, the EBF rate was minimally changed between 37 to 41 weeks of gestational age, with the highest at 40 weeks of gestational (58%) and the lowest at 36 weeks of gestational age (32%). In contrast, at Lakeside Hospital, EBF rates generally increase from 36 to 41 weeks of gestational, peaking at 41 weeks of gestational (88%) and at lowest at 36 weeks of gestational age (33%). A chi-square test comparing the EBF rate across the gestational week between Bergan and Lakeside showed an association between the EBF rate between the two hospitals. Further, chi-square tests comparing each gestational week between Bergan and Lakeside showed a significant association at 38, 39, 40, and 41 weeks. The results demonstrate that gestational age significantly impacts EBF rates. Notably, EBF rates at 36- and 37-weeks' gestation were similar but fell below CSH expectations.

Conclusion: Common Spirit Health's (CSH) goal of achieving 65% EBF for neonates in newborn nurseries has yet to be met by either hospital, with Bergan failing to meet the target at any gestational age. In contrast, Lakeside achieved the goal for neonates between 38 and 41 weeks but did not meet expectations for those born before 38 weeks. These findings underscore the need for further investigation into factors influencing EBF success, despite both hospitals providing education and consultation on lactation and breastfeeding for mothers. Maternal factors, such as age, delivery type, health conditions, breastfeeding education, and breast milk availability may play critical roles. Further exploration of these variables is essential to enhance understanding of this trend and to, ultimately, formulate strategies to improve EBF rates at both Bergan and Lakeside.

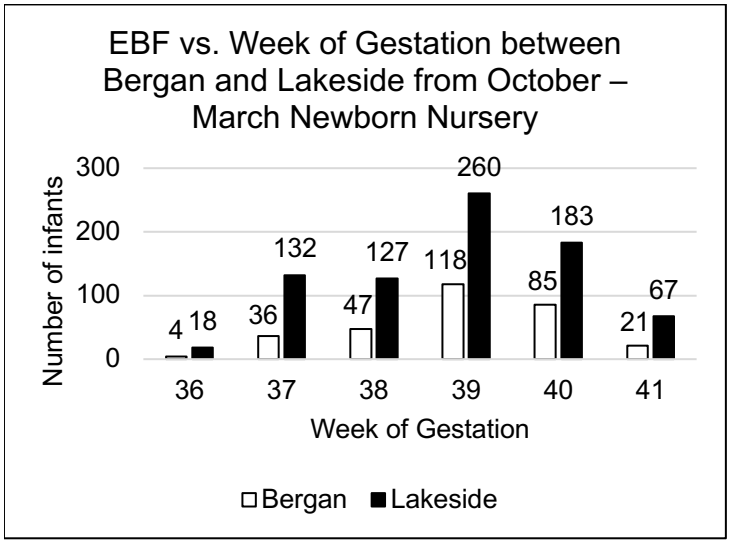

Figure 1. Number of infants receiving EBF vs. Week of gestation between Bergan and Lakeside from October-March in newborn nursery

Percent EBF From October to March		
Week	**Bergan**	**Lakeside**
36	32%	33%
37	50%	52%
38	54%	68%
39	52%	65%
40	58%	83%
41	54%	88%

Table 1. Percent EBF at each gestation age week at Bergan and Lakeside from October to March

SUPEROXIDE DISMUTASE-MIMETIC (BMX-001) AS A NOVEL ANTIOXIDANT THERAPY IN ALCOHOL-ASSOCIATED LIVER DISEASE

Delia Omar[1], Saumya Bhatt[1], Mathilda Willoughby[1], Kelly Otakhor[1], Todd Wyatt[1], Becky Deegan[1], Micah B. Schott[1]
[1]University of Nebraska Medical Center, Omaha, NE

Background, Significance and Hypothesis: Alcohol-associated liver disease (ALD) is a growing public health concern. Hepatic steatosis represents the earliest stage of ALD and is marked by lipid droplets (LDs) accumulation within hepatocytes, which are central for ALD progression. Additionally, hepatocytes accumulate reactive oxygen species (ROS) following ethanol (EtOH) metabolism, which then reacts with free fatty acids, leading to increased lipid peroxidation. However, it is unclear whether ROS can be targeted therapeutically to decrease lipid peroxidation. A promising antioxidant therapy for ALD is the superoxide dismutase SOD-mimetic (BMX-001), a lipophilic manganese porphyrin that scavenges excess intracellular ROS. BMX-001 is currently in several clinical trials against radiation-induced ROS damage. Moreover, pharmacokinetics data showed that BMX-001 stably accumulates within mouse livers in a dose dependent manner. However, its efficacy to delay ROS-driven hepatocyte damage in ALD has not been explored. For that, investigating the impact of ROS scavenging by BMX-001 as an antioxidant therapy for ALD to protect against lipid peroxidation is of great interest.

Experimental Design: C57BL6 mice were subjected to a diet enriched in polyunsaturated fatty acids (PUFA) with a chronic 10-day EtOH followed by a single binge of EtOH vs an isocaloric control PUFA diet with a single binge of maltose dextrin. Using this model, which is a better substrate for ROS-induced lipid peroxidation, mice were randomly assigned to four groups: Control + PBS, Control + BMX-001, EtOH + PBS, EtOH + BMX-001, and the drug administered by intraperitoneal injection (IP). At 6 hours post binge, mice were euthanized, liver tissue and blood serum were collected for subsequent analysis.

Results: Primary findings demonstrated an increase in the liver/body weight ratio in EtOH vs control PBS-treated groups (P-value 0.014), while no significant difference appeared in mice treated with BMX-001. Blood serum analysis revealed a significant elevation of Alanine Aminotransferase (ALT) liver injury marker in EtOH compared to the control PBS-treated groups (P-value 0.0152), while ALT levels are not remarkably changed between groups with BMX-001 treatment. Liver injury analysis based on gender revealed that female mice had significantly higher ALT levels in EtOH diet in both placebo (PBS) and BMX-001-treated groups (P-value 0.0286), while this difference was not observed in male mice.

Conclusions: EtOH-PUFA diet significantly increased liver/body weight ratio and elevated ALT levels, as a marker of induced-liver injury. Data suggest that female mice may be more prone to liver damage induced by EtOH compared with male mice. The non-remarkable changes in the liver injury marker and liver/body weight ratio between BMX-001-treated control and EtOH groups highlight the potential therapeutic effect of BMX-001 as a promising antioxidant in ALD. Histological assessment of liver tissues are ongoing to detect lipid peroxidation using a 4-HNE antibody, as well as steatosis using a PLIN2 antibody, to better elucidate the therapeutic effect of BMX-001 in ALD.

THE ROLE OF ECDYSONELESS, A NOVEL ESTROGEN-REGULATED PROTEIN, IN ESTROGEN RECEPTOR-POSITIVE BREAST CANCER

Farshid Oruji, Asher Rajkumar Rajan, Mohsin Raza, Bhopal Mohapatra, Hamid Band, Vimla Band (University of Nebraska Medical Center, Omaha, NE)

Background: Breast cancer (BC) is a heterogeneous disease, with estrogen receptor-positive (ER+) BC constituting over 70% of cases. ER+ BC relies on estrogen signaling for oncogenesis and metastasis. Despite advances in ER-targeted therapies, the molecular drivers of ER+ BC progression, particularly in metastatic stages, remain poorly understood. The expression levels of Ecdysoneless (ECD), a novel cell cycle and cell survival regulator, correlates with ER expression. ECD is overexpressed in ER+ BC and elevated ECD levels are associated with short survival in patients. This study investigates the interplay between ECD and ER, as well as ECD's role in ER+ BC oncogenesis.

Significance of Problem: Understanding the role of ECD, a novel ER-regulated gene in ER+ BC may reveal a new molecular pathway that could be a potential biomarker for ECD-targeted therapeutic for ER-dependent metastatic disease.

Hypothesis: Based on our novel findings, we hypothesize that ER regulated ECD overexpression in BC drives BC progression and metastasis. Thus, we posit that direct genetic or indirect pharmacological inhibition of ECD will negate the ECD overexpression-dependent pro-oncogenic and pro-metastatic drive-in ER+ BC.

Methods: Bioinformatic analysis of publicly available datasets was performed to explore the relationship between ER and ECD, including survival analysis linking ECD and ER expression. Chromatin immunoprecipitation (ChIP) and promoter-luciferase assays were employed to assess estrogen-dependent recruitment of ER to the ECD promoter. Estradiol (E2) treatment of cells was carried out to evaluate the effects of estrogen signaling on ECD expression. Functional assays in ER+ BC cell lines were performed to assess alterations in tumorigenic traits upon ECD overexpression.

Results: ECD expression positively correlated with ER levels in bioinformatic analyses. Elevated ECD levels were associated with short survival in ER+ BC patients. The ECD promoter contained estrogen response elements, and ChIP assays confirmed E2-mediated recruitment of ER to the ECD promoter. E2 treatment enhanced ECD promoter activity in luciferase assays. Overexpression of ECD in ER+ BC cells increased *in vitro* oncogenic traits.

Conclusions: ECD is a novel estrogen-regulated protein that promotes ER-driven oncogenesis in ER+ BC. These findings suggest ECD as a potential biomarker for ECD-targeted therapy. Ongoing studies are investigating ECD's role in *in vivo* oncogenesis and metastasis.

PROFILING THE CLINICAL COURSE OF NEWBORNS TREATED WITH THERAPEUTIC HYPOTHERMIA WITH MINIMAL OR NO METABOLIC ACIDEMIA

Michaela Palmer, Elizabeth R. Lyden, Eric S. Peeples (Benedictine College Atchison, KS)

Background, Significance, Hypothesis: Neonatal hypoxic-ischemic encephalopathy (HIE) occurs as a result of decreased oxygen and blood delivery to the brain around the time of birth. About 1 to 3 in 1,000 babies are diagnosed with HIE every year in high-income countries, and 40-60% of babies diagnosed with moderate to severe HIE will die or develop severe disabilities. Treatment for HIE with therapeutic hypothermia is most effective if initiated within the first six hours of life, and accurate diagnosis within that time frame can be difficult, as initial clinical indicators are often non-specific. Blood metabolic acidemia –defined in this population as pH<7.1 and base deficit >12 – is currently the most reliable laboratory biomarker for diagnosis. However, significant blood acidemia is not always present at the time of delivery, despite the presence of tissue acidosis, further complicating the ability to diagnose the neonate for treatment within the proper window of time. We hypothesized that by babies with HIE presenting with and without acidemia would have separate distinct phenotypes.

Experimental Design: This was a case-control study of newborns admitted to the neonatal intensive care units at Nebraska Medical Center and Children's Nebraska. Neonates included were born at ≥35 weeks of gestation, diagnosed with HIE, and treated with therapeutic hypothermia. Blood gas information and other lab results such as lactate, aspartate aminotransferase (AST), and alanine aminotransferase (ALT) measurements obtained within the first 24 hours of life and recorded. Subjects were stratified into two groups based on the presence of blood acidemia in umbilical cord blood gas or initial baby gas at <1 hour of life. Clinical magnetic resonance imaging (MRI) interpretations from the neuroradiologist were translated into binary findings of presence/absence of HIE-related brain injury.

Data and Results: Cord, initial, and trough baby pH were all lower in the acidemia group (p<0.001 each), and the initial and peak base deficits were higher in the acidemia group (p<0.0001) compared to the no acidemia group. The no acidemia group displayed elevated median initial and peak lactate concentrations when compared to normal concentrations (median 3.3 mmol/L, range 1.2-14.5 initial and median 3.8, range 1.7-14.5 peak). Peak AST values were significantly higher in the acidemia group compared to the no acidemia group (median 127.00, range 24.00-6545.00 vs. median 89.00, range 37.00-423.00, respectively, p=0.0499; Fig. 1). There was a small and likely clinically insignificant difference in 10-minute Apgar scores between groups (p=0.039).

Conclusion: In our single-center study, we were not able to identify a distinct phenotype in the no acidemia group. Median initial and peak lactate concentrations were higher in the acidemia group; however, although lower than the acidemia group, the no acidemia group lactate concentrations were elevated above normal. Since MRI findings can differ based on timing of injury, further investigation could include assessing differences in specific MRI findings.

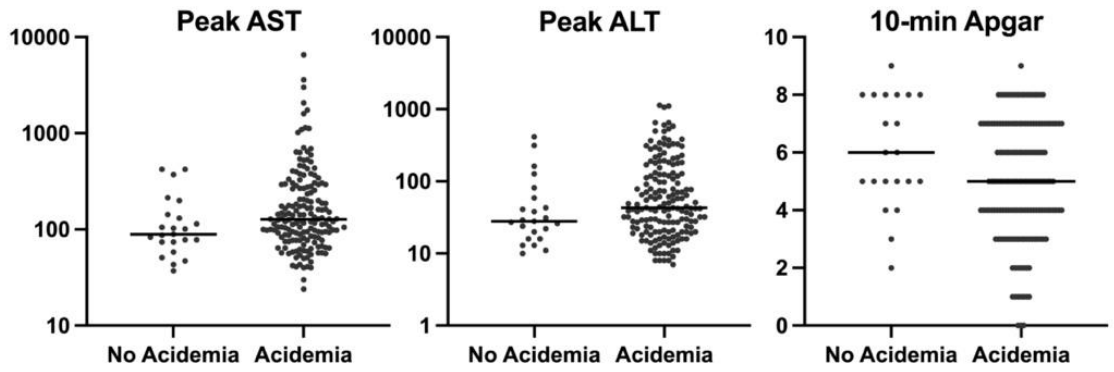

Figure 1. Higher peak aspartate aminotransferase (AST, p=0.049) and lower 10-minute Apgar score (p=0.039) in acidemia group. No difference in peak alanine aminotransferase (ALT).

COMBINED EFFECTS OF GABAPENTIN WITH VERAPAMIL AND METOPROLOL ON CARDIOVASCULAR FUNCTION OF ANESTHETIZED RATS

Sarah Pribil Pardun[1], Spencer Duff [1], Ian Papenfus[1], Will Bruening[1], Yulong Li[1], Gurudutt Pendyala[1], Lie Gao[1]

[1]University of Nebraska Medical Center, Omaha, NE

* Correspondence: lgao@unmc.edu (G.L.)

Abstract

Gabapentin (GBP) has been shown to negatively affect the cardiovascular system, inducing bradycardia, hypotension, and impaired left ventricular (LV) function in rats. However, its interaction with other cardiovascular medications remains unclear. This study investigates the combined effects of GBP with Verapamil (Ver) or Metoprolol (Met) on cardiovascular function in anesthetized rats. Twenty-two male Sprague Dawley rats were divided into four groups: Saline + Ver, GBP + Ver, Saline + Met, and GBP + Met for two experiments. Under 2% isoflurane anesthesia, rats were equipped with electrocardiogram (ECG) leads, Millar pressure transducers for LV hemodynamics and blood pressure (BP) measurements, and a femoral vein catheter for drug administration. Rats received an intravenous injection of GBP (50 mg/kg), followed by four doses of Ver (0.05, 0.1, 0.2, and 0.4 mg/kg) or one dose of Met (0.5 mg/kg). In the first experiment, Ver induced a dose-dependent reduction in BP, heart rate (HR), and maximal dP/dt, while increasing minimal dP/dt in both control and GBP-treated groups. GBP-treated rats exhibited a larger drop in BP compared to saline controls, especially at higher Ver doses. For HR and LV function, GBP exerted greater inhibitory effects, particularly at lower Ver doses. In the second experiment, GBP significantly reduced BP, HR, and maximal dP/dt while increasing minimal dP/dt compared to baseline. These effects were further exacerbated by Met, leading to greater reductions in BP, HR, and maximal dP/dt, and increases in minimal dP/dt compared to Met alone. These findings suggest that GBP enhances the negative chronotropic, negative inotropic, and hypotensive effects of both Ver and Met. Clinically, patients on GBP may need to consider lowering the doses of calcium channel blockers or beta-1 blockers.

Key Words Gabapentin; Verapamil; Metoprolol; Cardiovascular Function; Rats

DISPOSITION OF PATIENTS AND LENGTH OF STAY FOR INITIAL TRACHEOSTOMY IN NEBRASKA

Taylor Pitzl, Jayme R. Dowdall, Kaeli Samson, Jana Wardian, Dan Pierce
University of Nebraska Medical Center College of Medicine, Omaha, NE

Background and Significance of Problem

Midwestern tracheostomy patients face excess length of stay (LOS) which increases healthcare costs. The reasons for these prolonged stays have not been well described. Hospitals need to counsel patients, families, and care coordinators regarding realistic anticipated time in the hospital and available post-hospital care options to align with patient and family goals of care.

Hypothesis

We hypothesize that excess length of stay for tracheostomy patients may be due to several factors including discharge disposition and insurance status.

Experimental Design

This study was performed as an IRB-approved retrospective chart-review. 353 records of patients undergoing initial tracheostomy placement in Nebraska were reviewed for LOS, discharge delays and disposition. Discharge delay was defined as the patient remaining in hospital for 3 or more days after being deemed medically stable for discharge (MSD). Data are summarized with medians and interquartile ranges (IQRs).

Results

18.2% of patients were decannulated and 16.8% expired prior to discharge. Of the 65% remaining patients discharged with tracheostomy, 26% faced increased LOS after being medically stable for discharge with the median LOS of 14 days after tracheostomy placement. Post hospital discharge includes Acute Rehab Facility 40 (11.4%) Home 44 (12.5%), Hospice 9 (2.6%), Long Term Acute Care (LTAC) 123 (34.9%), Prison 1 (0.3%). Skilled Nursing Facility (SNF) 4 (1.1%).

Specific facilities, such as prison, long-term care and SNF were associated with increased LOS. SNF LOS varied widely from 1.5- 81 days after medically stable for discharge. When experiencing a delay due to insurance authorization, 78% were delayed for more than 3 days after MSD. 24.9% of discharge locations were discrepant between manual review and EHR report.

Conclusions

Improved understanding of LOS, timeline, and disposition of tracheostomy patients can lead to better planning. Early discharge planning could potentially minimize avoidable hospital days.

UNDERSTANDING BARRIERS TO PELVIC FLOOR PHYSICAL THERAPY ADHERENCE IN MALES WITH PELVIC FLOOR DYSFUNCTION

Janani Raman, Clare M. Wieland, Katie Shalon, Dannie B. Dilsaver, Joan C. Delto (Creighton University Omaha, NE)

Background, Significance, Hypothesis: Pelvic floor dysfunction (PFD) is a broad collection of symptoms and anatomical changes that result in improper coordination of the pelvic floor musculature and supporting organs. Pelvic floor physical therapy (PFPT) is an underutilized effective treatment option for male patients experiencing PFD. Early intervention via PFFT has shown to hasten recovery times post urological surgery for males with PFD. Barriers that men face with PFPT adherence are severely under-researched. No studies thus far have addressed factors that affect adherence in men with PFD. Poor adherence to PFPT has negative outcomes for treatment cost and effectiveness. This is a pivotal area of research that may improve treatment outcomes for patients experiencing PFD in the future. The aim of this study was to assess possible barriers associated with PFPT adherence.

Experimental Design: From December 2023 to June 2024, male patients 19 years and older with PFD who were referred to CHI Pelvic Health Centers were surveyed about their opinions and experience with PFPT. Patient characteristics were stratified by adherence and compared via Fisher's exact and independent-samples t-test.

Data and Results: 77 patients were included in the study; 64.9% attended at least one PFPT visit. Irrespective of PFPT adherence, 79.2% (N=61) of patients stated they had no therapist gender preference. Of those non-adherent to PFPT, 44.4% (N=12) stated that they were not informed or partially informed about PFPT. Relatedly, a majority of the non-adherent group was uninsured and reported cost concerns compared to the adherent group (Table 1). Patient emotional limits and willingness to spend time doing PFPT exercises did not vary by adherence (Table 1).

Conclusion: Financial concerns and lack of prior education about PFPT were notable factors limiting PFPT adherence. Importantly, the majority of patients believed in the importance of preventative health (irrespective of adherence). Considering patient perceptions (before and after) related to PFPT will help clinicians and physical therapists tailor patient discussions to promote better understanding of and adherence to treatment recommendations.

Table 1. Patient preferences and factors stratified by adherence to pelvic floor physical therapy

	Adherence		Total (N=77)	p
	No	Yes		
Education, n (%)				
Highschool	7 (25.9%)	10 (20.0%)	17 (22.1%)	0.080
Some college	5 (18.5%)	12 (24.0%)	17 (22.1%)	
Undergraduate degree	7 (25.9%)	12 (24.0%)	19 (24.7%)	
Graduate degree	4 (14.8%)	13 (26.0%)	17 (22.1%)	
General Education Development	4 (14.8%)	0 (0.0%)	4 (5.2%)	
Health Insurance, n (%)	24 (88.9%)	50 (100.0%)	74 (96.1%)	0.040
Cost Issue, n* (%)	10 (43.5%)	9 (18.8%)	19 (26.8%)	0.044
PFPT Defined, n (%)				
Not informed	6 (22.2%)	1 (2.0%)	7 (9.1%)	< 0.001
Partially informed	6 (22.2%)	2 (4.0%)	8 (10.4%)	
Well informed	15 (55.6%)	47 (94.0%)	62 (80.5%)	
Prevention, n (%)				
Not Important	0 (0.0%)	2 (4.0%)	2 (2.6%)	0.162
Possibly Important	3 (11.1%)	3 (6.0%)	6 (7.8%)	
Important	11 (40.7%)	11 (22.0%)	22 (28.6%)	
Very Important	13 (48.1%)	34 (68.0%)	47 (61.0%)	
Weekly Time PT, n (%)				
Less than an hour	13 (48.1%)	20 (40.0%)	33 (42.9%)	0.210
1-2 hours	9 (33.3%)	14 (28.0%)	23 (29.9%)	
2-3 hours	1 (3.7%)	10 (20.0%)	11 (14.3%)	
4+ hours	3 (11.1%)	6 (12.0%)	9 (11.7%)	
Other	1 (3.7%)	0 (0.0%)	1 (1.3%)	
Travel Distance, n* (%)				
Less than 5 miles	9 (64.3%)	22 (44.9%)	31 (49.2%)	0.560
5-10 miles	4 (28.6%)	21 (42.9%)	25 (39.7%)	
10+ miles	1 (7.1%)	6 (12.2%)	7 (11.1%)	
PFPT Perceptions Before, n* (%)				
Might be helpful	8 (30.8%)	25 (50.0%)	33 (43.4%)	<.0001
Helpful	7 (26.9%)	22 (44.0%)	29 (38.2%)	
Not Helpful	0 (0.0%)	3 (6.0%)	3 (3.9%)	
Did not attend	11 (42.3%)	0 (0.0%)	11 (14.5%)	
PFPT Perceptions After, n* (%)				
Might be helpful	1 (4.2%)	4 (8.3%)	5 (6.9%)	<.0001
Helpful	0 (0.0%)	40 (83.3%)	40 (55.6%)	
Not Helpful	0 (0.0%)	4 (8.3%)	4 (5.6%)	
Did not attend	23 (95.8%)	0 (0.0%)	23 (31.9%)	
Preferred Time, n* (%)				
Morning	7 (25.9%)	23 (46.9%)	30 (39.5%)	0.294
Mid-morning	11 (40.7%)	12 (24.5%)	23 (30.3%)	
Early afternoon	5 (18.5%)	8 (16.3%)	13 (17.1%)	
Late Afternoon	4 (14.8%)	6 (12.2%)	10 (13.2%)	
Gender Preference, n (%)				
Male	3 (11.1%)	0 (0.0%)	3 (3.9%)	0.006
Female	1 (3.7%)	12 (24.0%)	13 (16.9%)	
No preference	23 (85.2%)	38 (76.0%)	61 (79.2%)	
Emotional Limits, n* (%)				
None	18 (90.0%)	46 (95.8%)	64 (94.1%)	0.575
Somewhat	2 (10.0%)	2 (4.2%)	4 (5.9%)	

An * indicates some participants were missing a response, percent is out of those who responded.
PFPT = pelvic floor physical therapy
PT = physical therapy

TRENDS IN ACUTE PANCREATITIS-RELATED MORTALITY IN THE UNITED STATES (1999-2022): A COMPREHENSIVE ANALYSIS USING THE CDC WONDER DATABASE

Maya M. Samuel, Austin M. Veire, Vikram Murugan, Taylor Billion, Abubakar Tauseef (Creighton University, Omaha, NE)

Background, Significance, Hypothesis: Acute pancreatitis is one of the most prevalent gastrointestinal diseases requiring hospital admission in the United States. The reported annual incidence of acute pancreatitis in the United States is currently 40/100,000 people which accounts for over 270,000 hospitalizations each year. From 1999-2022, there were 141,856 deaths due to acute pancreatitis in the United States. Characterizing the trends in acute pancreatitis related mortality is crucial to improving health outcomes in the United States.

Experimental Design: This study utilizes the CDC WONDER database to analyze trends in acute pancreatitis mortality across the U.S. from 1999 to 2022. Mortality attributed to acute pancreatitis was identified using the International Classification of Diseases, 10th Revision, Clinical Modification codes K85 in patients ≥ 15 years. Data on demographic and regional groups were extracted, which included gender, race/ethnicity, age, urban-rural classification, and geographic region. Age groups were defined in 10-year age intervals starting at 15 to 24 years through 85+ years of age. The Joinpoint Regression Program was used to identify significant changes in annual mortality trends over time. Annual percentage change (APC) with 95% confidence intervals (CIs) for the age-adjusted mortality rates (AAMR) were calculated for the line segments linking a Joinpoint using the Monte Carlo permutation test. The weighted average of the APCs were calculated and reported as average annual percentage change (AAPC) and corresponding 95% CIs as a summary of the reported mortality trend for the entire study period.

Data/Results: The overall average annual percentage change (AAPC) of age adjusted mortality rates (AAMR) was -0.787* from 1999-2022. AAMR was lowest at 1.85 (95% CI 1.80 to 1.90) in 2018. From 1999-2022, acute pancreatitis caused 62,257 (43.9%) deaths in females and 79,599 (56.1%) deaths in males in the U.S. The AAPC in AAMR was -1.240* for females and -0.536* for males in this time period. Black or African American people had the highest AAMR from 1999 to 2008, starting at 4.54 (95% CI 4.25 to 4.84) in 1999 and decreasing to 2.65 (95% CI 2.44 to 2.85) in 2008. However, from 1999-2015, the APC in AAMR for this population was -5.400* (95% CI -6.94 to -4.42), which was the largest decrease among all populations studied. From 2009-2022, American Indians and Alaska Natives had the highest overall AAMR and continued to increase from 3.60 (95% CI 2.62 to 4.83) in 2009 to 4.97 (95% 3.99 to 6.11) in 2022. From 2011-2022, the APC in AAMR of American Indians and Alaska Natives was 6.100* (95% CI 3.06 to 19.73). Asian and Pacific Islanders had the lowest overall AAMR throughout the studied time frame. When comparing populated regions, AAMRs were consistently highest in rural areas than in metropolitan regions. In each year from 1999-2022, the South and the Midwest had the highest and second highest AAMR among census regions. In general, the Northeast had the lowest AAMR across all years. Across all years, the crude mortality rate was directly correlated with higher age. In 2020, there was an increase in crude mortality rates across all age groups.

Conclusions: Acute pancreatitis is a prevalent gastrointestinal disease that continues to affect individuals, with a substantial impact on mortality in the U.S. A comprehensive analysis of mortality trends in the U.S. show higher rates of acute pancreatitis related mortality in older individuals, males, American Indian and Alaska Natives, rural areas, and the South and Midwest census regions. Furthermore, there was an increase in crude mortality rates among all age groups in 2020. This phenomenon could be attributed to the emergence of COVID-19 but further studies are needed to establish this correlation.

IDIOPATHIC SCOLIOSIS IS NOT ACCURATLY IDENTIFIED BY ICD CODES ALONE

Taylor K, Yoshida C, Graham S, Smith H, Lange E, Johnson RK, Miller NH, Carry PM
(Creighton University, Omaha, NE)

Background, Significance of Problem, Question
We conducted a clinical chart review to assess disease prevalence and identify misclassification of Idiopathic Scoliosis (IS) based on International Classification of Diseases (ICD) codes assigned by the patient's provider. IS, a lateral curvature in the spine, presents in adolescence and affects 1-3% of general population. In our review, IS was defined as a Cobb angle greater than 15 degrees, excluding cases caused by congenital, syndromic, neuromuscular, traumatic, or infectious conditions. With the misclassification of diseases, there can be over reported disease prevalence leading to bias in treatment and resource allocation. There can also be insurance reimbursement issues, mistrust of the patient after an improper diagnosis, and hindered advances in treatment. The goal of the study was to understand the misclassification of IS based on ICD codes and to analyze demographic data of the confirmed cases of idiopathic scoliosis after extensive chart review.

Experimental Design
We identified all patients who were ≤50 years of age at a UCHealth system clinic visit and had one or more ICD (ICD9 and/or ICD10) scoliosis codes. We randomly selected n=2000 patients for manual chart review. We compared the distribution of demographics and clinical characteristics between the IS patient group versus the non-IS/no scoliosis patient group. Chi-square of reviewer's t-test were used to test for differences in these variables between the two groups.

Results/Data
Among the n=2,000 patients selected for chart review we excluded patients for the following: deceased at the time of chart review n=19, scoliosis diagnosis codes included in chart but diagnosis dates missing for all scoliosis codes n=285, and/or missing radiographs n=9. Among the n=1687 patients meeting the inclusion criteria, 34.9% (588/1687) met our diagnostic criteria for idiopathic scoliosis. Spinal asymmetry defined as a cobb angle 5-15 degrees, presence of syndromic scoliosis, and presence of neuromuscular scoliosis were the most prevalent reasons for classifying patients as non-idiopathic. Female biological sex, diagnostic imaging type, age when a scoliosis code was first documented in the chart, number of radiographic images, number of unique scoliosis diagnosis codes and number of unique visits in which a scoliosis code was documented was significantly different between the IS cases versus the non-IS/no scoliosis group indicated by p-value <0.05.

Conclusions
Analysis revealed that only 34.9% of idiopathic scoliosis cases were accurately coded using ICD classifications. This finding highlights the need for further research to assess misclassification on a larger scale, enabling a clearer understanding of the true disease prevalence and more precise demographic insights. It also emphasizes the need for thorough imaging review and clinical expertise to identify complex phenotypes.

SMALL MOLECULE DRUG DISCOVERY TO TREAT GLOBAL CEREBRAL ISCHEMIA THROUGH TREM1 INHIBITION

Prerna L. Tiwari[1]; Hyunha Kim[1]; Rachael Urquhart[1]; Peter Abel[1]; Gopal Jadhav[1]; Jee-Yeon Hwang[1]

[1]Department of Pharmacology and Neuroscience, Creighton University School of Medicine, Omaha, Nebraska, 68178.

Stroke is the second-leading cause of death, and the third-leading cause of death and disability combined in the world. Ischemic stroke constitutes the greatest proportion of strokes, and accounts for 75-85% of all strokes. Global cerebral ischemia, a severe form of stroke often caused by cardiac arrest, leads to cognitive deficits or death. While emergency treatments focus on restoring cardiac function, there is no effective treatment for neurodegeneration and cognitive impairment. TREM1, a membrane immune receptor, amplifies proinflammatory responses and contributes to neuroinflammation. Our recent studies showed that global ischemia activates TREM1 in the hippocampal CA1 in rats, and its inhibition by the peptide LR12 affords neuroprotection. Therefore, we hypothesize that TREM1 inhibition is a promising therapeutic strategy for global ischemia. However, current inhibitors have limitations including poor cell permeability and short half-life. To address these issues, we identified a N4-(amino-substituted)-N-substituted-benzenesulfonamide pharmacophore (hit molecule), using molecular docking of 80,000 molecules to the hTREM1 crystal structure (PDB: 1SMO). Surface plasmon resonance confirmed the hit molecule's affinity to TREM1, with a Kd of 14.3 μM. However, we observed some solubility issue with the hit molecule. To overcome this, we synthesized a fluoro-analog, GJ079, which exhibited significantly improved affinity to TREM1 (Kd = 4.8 nM) and enhanced solubility. We further showed that GJ079 attenuates global ischemia-induced neuroinflammation and neuronal death *in vivo*, demonstrating its neuroprotective potential. In addition, GJ079 decreased mRNA levels of TREM1 signaling related downstream factors, including pro-inflammatory cytokines, indicating that it effectively rescues the TREM1-mediated inflammatory response. Based on these findings, we hypothesize that structural modifications to the hit molecule could lead to development of non-toxic, bioavailable, and potent TREM1 inhibitors. Toward this end, we synthesized 45 hit molecule-based analogs in five series, with structural modifications to improve solubility and affinity: Series 1 required an additional aromatic-acetamido substitution on a thiazolyl group containing nitrogen of 4-amino-N-(thiazol-2-yl) benzenesulfonamide; Series 2 involved an aromatic-acetamido substitution on the N4- aromatic amino group; Series 3 featured ortho, meta and para fluoro substitution on the end phenyl ring of GJ079; Series 4 involved the replacement of the 2-thiazolyl ring with another hetero aromatic ring in the GJ079; and Series 5 with aromatic-amido substitution on the N4- aromatic amino group. For biological validation, we are currently testing the ability of these compounds to inhibit TREM1 activity using a stable NFAT_luc_TREM1/DAP12 HEK293 cell line. Lead compounds will undergo pharmacokinetic assays and be tested in both *in vitro* and *in vivo* models of global ischemia to confirm their therapeutic potential.

EVALUATING FLINT HILLS PRESCRIBED BURN EMISSIONS AND PEDIATRIC ASTHMA EXACERBATIONS IN DOUGLAS COUNTY, NE

Authors: Denise Torres[1], Kelli Gribben, Jagadeesh Puvvula, Yeongjin Gwon, Jill Poole, Azar Abadi, Jesse Bell

1. University of Nebraska Medical Center College of Medicine, Omaha, NE

Background, Significance, Hypothesis: Several studies suggest that exposure to air pollution from prescribed burn emissions potentially increase health burden, especially for respiratory-related causes. Prescribed burning, averaging 2.1 million acres with an estimated 2,000-3,000 fires, occurs annually in the Flint Hills. A previous study done in Kansas found an increase in same-day asthma emergency department visits associated with prescribed burn smoke exposure, with the pediatric population having the highest frequency of asthma, respiratory, and cardiovascular emergency room visits. Impacts to Nebraska's air quality and potential health effects of Flint Hills prescribed burning are not well understood. This study investigates if annual prescribed burning in the Flint Hills is associated with an increased risk for an emergency department visit for an asthma exacerbation among children 0-19 years old living in Douglas County, NE. We hypothesized a positive association between Flint Hills prescribed burn emissions and pediatric asthma exacerbation related emergency department visits in Douglas County, NE. Understanding the health impacts of the Flint Hills prescribed burn emissions on Nebraska populations would help provide advisory warnings by identifying asthma risk during the prescribed burn season.

Experimental Design: A daily time-series analysis was performed to explore potential associations between levels of particulate matter with a diameter of 2.5 micrometers or smaller ($PM_{2.5}$) and other air pollutants during Flint Hills prescribed burn days with emergency department visits for an asthma exacerbation among the pediatric population (< 20 years) residing in Douglas County, NE during 2016-2019. The primary exposure was the daily maximum $PM_{2.5}$ ($\mu g/m^3$). Other air pollutants evaluated were PM_{10}, ozone, carbon monoxide, sulfur dioxide, nitrogen dioxide, nitric oxide, and nitrogen species. Air pollution data were measured at a single station monitor at the Douglas County Health Department and obtained from the US EPA Air Quality System (AQS). Information on prescribed burns was obtained from the Kansas Department of Health and Environment, including dates and number of acres burned. These dates were aggregated to define prescribed burn and non-prescribed burn periods. Daily meteorological data were retrieved from NOAA Global Historical Climatology Network Daily (GHCNd) with measurements from the station at Omaha Eppley Airfield. The health outcome data, daily pediatric asthma emergency department (ED) visits (ICD-10-CM J45), were obtained from the Nebraska Hospital Association, with only patient age and sex available in the dataset. Environmental data were merged with health outcome data using dates. Descriptive statistics and plots were produced, and a Quasi-Poisson regression model was fit to evaluate relationships between daily $PM_{2.5}$ and number of ED visits for a pediatric asthma exacerbation stratified by prescribed burn day (yes/no). We performed sensitivity analyses examining the interaction between $PM_{2.5}$ prescribed burn day (y/n) and lagged effects 0-5 days in both full and stratified analyses. Covariates included seasonality (time modeled as cubic B spline), daily temperature, and wind speed (meters/sec). Analyses were conducted in R and SAS. Study was approved by UNMC IRB.

Results/Data: There were 264 days where prescribed burning occurred and 1,178 non-burn days during 2016-2019. There was a total of 4,744 ED visits for a pediatric asthma exacerbation, majority male and aged 0-5 years. No associations were found between Douglas County, NE $PM_{2.5}$ levels and ED visits for a pediatric asthma exacerbation during the Flint Hills prescribed burn days during the four-year study period.

Conclusions: We did not find any associations between Douglas County, NE $PM_{2.5}$ levels and ED visits for a pediatric asthma exacerbation during the Flint Hills prescribed burn days during our study period. Some limitations to our study include $PM_{2.5}$ measurement coming from a single monitor to represent the whole county, inability to attribute $PM_{2.5}$ to prescribed burn smoke, unmeasured time-varying confounders, and not knowing the asthma status of patient population. A longer time series may be required, in addition to air quality data covering a larger geographic area to better evaluate potential impacts of Flint Hills prescribed burning to Nebraska communities.

OPTICAL MEASUREMENTS OF GLUTAMATE RELEASE FROM ROD PHOTORECEPTOR CELLS IN MOUSE RETINA

Lou Townsend, Channabasavaiah Gurumurthy, Wallace B. Thoreson
University of Nebraska Medical Center, Omaha, NE

Background:
Vision is initiated by the capture of photons by rod photoreceptor cells in the retina. Rod light responses are transmitted to second-order bipolar and horizontal cells by changes in the ongoing rate of synaptic release of glutamate. Synaptic transmission from rods has traditionally been studied using electrophysiological techniques, but these techniques have limited ability to study release from multiple individual neurons simultaneously. Published electrophysiological data shows evidence that glutamate release from rods in darkness occurs at regular intervals. To confirm these surprising results, we propose to measure glutamate optically using a fluorescent reporter. To do so, we generated genetically modified mice that express the glutamate sensor iGluSnFr3.v857.GPI specifically in rods.

Significance of Problem:
The rate of release, diffusion, and re-uptake of glutamate in the synaptic cleft shapes transmission and our ability to see. Releasing vesicles at regular rather than random intervals can improve detection of dim lights at visual threshold. This new mouse model can also be adapted for studying changes in glutamate release in retinal degeneration and disease.

Hypothesis:
We hypothesize that glutamate release from rods occurs at regular, not random, intervals.

Experimental Design:
Rod-specific iGluSnFr3: Using EasiCRISPR methodology, the UNMC Genome Engineering core generated mice that selectively express iGluSnFr3 in rods with expression driven by the promoter for a rod-specific gene, rhodopsin. We chose a variant that couples to the membrane via GPI-linkage for improved synaptic expression. We use heterozygous mice that express a normal rhodopsin gene along with the iGluSnFr3. Electroretinograms (ERGs) were recorded from anesthetized mice using a gold corneal electrode and ganzfeld illuminator (LKC, Gaithersburg, MD).

For imaging, living retinas were placed on a slide and superfused with oxygenated Ames' medium at 37 deg C. Cone photoreceptor cell terminals located just proximal to rod synapses are labeled with peanut agglutinin (PNA)-conjugated rhodamine to use as a landmark. Retinas were imaged on a two-photon confocal microscope (Scientifica). Fluorescence was measured with line scans that traversed individual rod terminals (2-5 ms/line). We calculated the power spectra of time-dependent fluorescence changes among individual rod terminals using ImageJ and Clampfit (Molecular Devices) software. Power spectra from different cells were averaged using a custom binning routine in R (RStudio).

Results/Data:
ERG A-waves that reflect photoreceptor light responses did not differ between wild-type and iGluSnFr3-expressing mice, consistent with prior evidence that a single copy of the rhodopsin gene is sufficient for normal responses. Line scans of rod terminals in darkness showed both rapid and slow fluorescence fluctuations. As expected for synaptic release, these fluctuations were increased by warming retinas from 23 to 37 deg. C and suppressed after inhibiting Ca^{2+} influx with the L-type Ca^{2+} channel blocker, nifedipine. To test if fluorescence changes arise from synaptic release, we co-loaded an activity-dependent dye, 10kD dextran-conjugated pHrodo. This dye fluoresces inside acidic synaptic vesicles but is quenched after release into the alkaline extracellular environment. Consistent with detection of release events, sharp peaks in iGluSnFr3 fluorescence coincided with troughs in pHrodo fluorescence. Power spectral analysis of line scans consistently show large changes in iGluSnFr3 fluorescence at low frequencies (<2 Hz) along with a second peak at 6-8 Hz (n = 61 rods) (Fig 1). Since randomly occurring release events would produce a flat power spectrum, these data are consistent with regular release.

Conclusions:
Our results show that this new iGluSnFr3-expressing mouse model is sensitive enough to detect release events in individual rods. The results also support the hypothesis that release occurs at regular intervals of 6-8 Hz. Lower frequency regularity may also be present, but measurements of low frequency changes are obscured by dye bleaching. Given ERG results showing that these mice exhibit normal rod light responses, we plan to test whether low frequency peaks in fluorescence power spectra are abolished by hyperpolarizing rods with a dim background light.

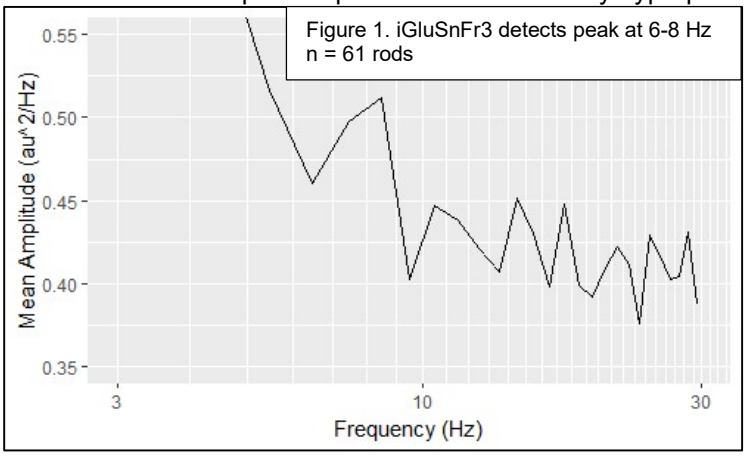

COMBINATORIAL TARGETING OF EXPORTIN 1 IN CUTANEOUS SQUAMOUS CELL CARCINOMA

Meghan Vo, Moynul Islam, Louise Monga, James A. Grunkemeyer, and Laura A. Hansen
Department of Biomedical Sciences, Creighton University School of Medicine, Omaha, NE

Background

Cutaneous squamous cell carcinoma is the second most common non-melanoma skin cancer with increasing incidence rates. Even though it accounts for 20% of cutaneous malignancies, it contributes to 75% of all non-melanoma skin cancer deaths. The Hansen lab has shown that the aberrant localization of proteins to cytoplasm contributes to an acquired pro-survival state of skin cancer cells. The nuclear export protein, XPO1, a major player in maintaining cellular homeostasis, is upregulated in several cancers. Selinexor is a selective XPO1 inhibitor that inhibits the survival of cSCC *in vitro*. Since XPO1 is essential in normal functioning cells, inhibiting its function in therapy has major systemic toxicities. In clinical trials where Selinexor was administered to patients with solid tumors, the treatment related adverse events from these trials show that systemic toxicity poses a major setback to using Selinexor as therapy. Thus, finding new targets for combination therapy with Selinexor may yield a treatment regimen that is more toxic to cSCC-13 cells than either drug alone. Additionally, topical treatment may enable a higher effective dose of the combination Selinexor/other when compared to systemic administration.

Using a genome-wide CRISPRi screen, the Hansen lab identified a list of genes that, when CRISPRi targeted, increase Selinexor's potency. *KAT2A* and *TKK* genes were chosen as potential inhibition targets based on their mean log-fold change and commercial availability of inhibitors. KAT2A is a histone acetyltransferase enzyme (Gcn5) that regulates gene expression. KAT2A is over-expressed in many cancers, increases cell proliferation, and increases tumor growth in mouse models. Because of its role in the pathogenesis of disease, many small molecule KAT2A inhibitors have been developed, including Butyrolactone and CPTH-6.

The second protein of interest is TTK kinase, also known as monopolar spindle 1 kinase (Mps1). TTK exerts its function during mitosis and is associated with poor prognosis in gastric and breast cancers. Empesertib is a selective TTK inhibitor shown to induce tumor cell death and synergize with paclitaxel.

Significance of Problem

The incidence of cutaneous squamous cell cancer is increasing in the United States with the southern and central regions having mortality rates that are comparable with renal and oropharyngeal carcinomas and melanoma. When radiation therapy or surgical excision are not viable options for locally advanced or metastatic cSCC, immune checkpoint inhibitors that target PD-1 and PD-L1 are currently the first line of treatments. Cemiplimab, a human monoclonal antibody that blocks PD-1, became the first FDA-approved treatment for advanced/metastasized cSCC. While adverse reactions to Cemiplimab remained between grade 1 and 2 during phase I and II clinical trials, the drug is not an option for organ transplant patients, who are on lifelong immunosuppressive drugs. For these patients, alternatives include targeted therapy, such as EGFR, or cytotoxic chemotherapy, such as carboplatin, cisplatin, or 5-FU. While cytotoxic chemotherapy is used in combination with radiation or surgery, its toxicities are still major barriers to a successful therapeutic outcome. Current studies show that more than one third of patients treated with cytotoxic chemotherapy in combination regimen have grade 3 to 4 hematologic adverse events, such as neutropenia, prompting the need to explore combination therapy and topical administration to treat cSCC with less side effects.

Hypothesis This project was designed to test the hypothesis that combining XPO1 inhibition via Selinexor with the inhibition of KAT2A or TTK will be more effective at killing cSCC cells than either drug alone.

Experimental Design

The IC_{25} and IC_{50} values for Butyrolactone, CPTH-6, and Empesertib were determined in cSCC cell line cSCC-13 by seeding cells at 8,000 cells/well in 96-well culture plates the day before drug treatment was initiated. The cells were treated with each inhibitor at 9 different concentrations in six replicate wells for 4 days, with media/inhibitor changed daily. A Resazurin assay was performed to determine the effects of the drugs on cell viability. For the combination treatment experiment, cSCC-13 cells were treated with the IC_{25} concentrations of Selinexor only, KAT2A or TTK inhibitor only, or with Selinexor + KAT2A or TTK inhibitor. The Resazurin Assay was used to determine the relative effects of each treatment condition at 24 hours intervals.

Results The IC_{50} of the inhibitors were 133 uM – 159.4 uM for Butyrolactone, 108.4 uM for CPTH-6, and 3.8 nM - 18.03 nM for Empesertib. Combinatorial experiments of Selinexor with Butyrolactone or Selinexor with Empesertib showed a nonsignificant increase in apoptosis when compared to either drug alone. shRNA knockdown of KAT2A also did not enhance Selinexor toxicity in cSCC-13 cells. Selinexor and CPTH-6 together did not increase apoptosis when compared with either drug alone.

Conclusion We found that cSCC-13 cells did not respond with more cell death to KAT2A and TKK inhibitors when combined with Selinexor. A possible explanation could be that Butyrolactone and CPTH-6 induce cell cycle arrest before the cells enter S-phase or mitosis, which is when Selinexor is most effective. To circumvent this complication in future experiments, we plan to treat cells with Selinexor before treating with the KAT2A or TTK inhibitors. Another approach would be to use inhibitors that target the cell cycle during mitosis when Selinexor is most active, such as survivin inhibitors.

IDENTIFICATION OF ARGININE TRANSPORTERS IN *STAPHYLOCOCCUS AUREUS*

Gabrielle Watson and Paul D. Fey

University of Nebraska Medical Center, Omaha, NE

Background

Staphylococcus aureus is a Gram-positive bacterium that colonizes approximately 30% of the population and causes infection in various host niches including the skin and soft tissue. Glycolytic activity is required to initiate a skin and soft tissue infection indicating that carbon catabolite repression (CCR) mediated by CcpA likely represses secondary carbon source metabolism, including that of many amino acids. Due to CcpA-mediated repression, *S. aureus* is an arginine and proline auxotroph in chemically defined medium containing glucose (CDMG). In the absence of glucose, arginine is an important carbon source. Within *S. aureus* USA300, two known arginine/ornithine antiporters, ArcD1 and ArcD2, are encoded on the two copies of the arginine deiminase operons. However, when both antiporters are inactivated, no growth defect is observed in chemically defined medium. This suggests *S. aureus* encodes additional arginine transporters.

Significance of Problem

S. aureus is the leading cause of skin and soft tissue infections (SSTI) which accounts for nearly 500,000 hospitalizations a year. Abscesses can form in the underlying deep tissue and rupture causing a release of bacteria in the surrounding tissue and blood. During the initiation of an infection arginine is located on the skin and in the bloodstream (50-150μM). Once an immune response is triggered various immune cells such as macrophages and T cells respond and rely on arginine from the milieu to kill pathogens and replicate efficiently. Both in a SSTI and in the blood, glucose is required to establish an infection indicating that arginine and proline biosynthesis is repressed via CCR. Several pathogens including *Listeria monocytogenes*, *Schistosoma mansoni*, and *Leishmania spp* exhibit an increase in arginine transporter transcription during infection.

Hypothesis

S. aureus encodes multiple arginine transporters that are critical for the establishment of an infection.

Experimental Design

To identify essential arginine transporters, we utilized the Nebraska Transposon Mutant Library (NTML) and suppressor screens using canavanine, a toxic arginine analog. All amino acid permeases from the NTML were screened in CDM lacking proline and glutamate (CDM-PE) where growth is dependent upon the transport of arginine. Those mutants with a reduced growth phenotype were further assessed for arginine transport function via growth analysis in various media conditions and growth in the presence of canavanine. In parallel, the *arcD1 arcD2* mutant was grown in the presence of canavanine, suppressor mutants were isolated and whole genome sequencing was performed to identify the location of single nucleotide polymorphisms (SNPs). Various growth conditions were tested to determine when SAUSA300_2383 is active. In addition, regulation of SAUSA300_2383 via AhrC and CcpA was assessed via RT-PCR. RNA sequencing and transport assays were performed to identify if additional arginine transporters are regulated via AhrC.

Results

Following the screening of amino acid permease mutants from the NTML, SAUSA300_2383 displayed reduced growth yields in CDM-PE. In addition, thirteen of the fourteen suppressor mutants resistant to canavanine had SNPs in the uncharacterized amino acid permease SAUSA300_2383. The permease appears vital in growth conditions lacking proline, especially in the presence of salt stress. Additionally, SAUSA300_2383 is repressed via CcpA in the presence of glucose and repressed via AhrC when glucose is no longer present. The *arcD1 arcD2 2383* mutant (triple mutant) still supported growth in CDM-PE, suggesting another arginine transporter is functional. When the *ahrC* mutant was introduced into the triple mutant there was an increase in growth, suggesting AhrC represses an additional arginine transporter. This is further indicated via transport studies, where the *ahrC* mutant displays increased arginine uptake compared to wildtype.

Conclusions

The protein encoded by SAUSA300_2383 was identified as a potential arginine transporter. An additional *S. aureus* arginine transporter is repressed vis AhrC.

Title: RELIABLITLITY OF THE MODIFIED CHECKLIST FOR AUTISM IN TODDLERS-REVISED (MCHAT-R) IN A NEONATAL INTENTIVE CARE UNIT (NICU) FOLLOW UP CLINIC

Emma Weis, Paige Hardy, Abbey Siebler, Kerry Miller, Howard Needelman,

University of Nebraska Medical Center, Omaha, Nebraska

Background, significance, and hypothesis: The Neonatal Intensive Care Unit (NICU) provides specialized care for 9-13% of infants at birth, addressing complex medical needs. NICU graduates are at an increased risk for developmental challenges, including autism spectrum disorder (ASD). ASD is typically screened for during 18- or 24-month well-child visits using the Modified Checklist for Autism in Toddlers-Revised (MCHAT-R), a 20-item parent-reported screening tool designed to identify developmental concerns.

While the MCHAT-R has demonstrated high predictive accuracy for ASD in full-term infants, its validity in NICU graduates remains uncertain. Current research highlights its limited predictive value in very preterm infants but lacks comprehensive evaluation across the diverse NICU graduate population, including full-term infants with complex medical histories.

This study aims to assess the predictive utility of the MCHAT-R in a broader NICU graduate cohort, and identify alternative factors that may enhance the early identification of ASD in this high-risk population. We hypothesize that the MCAT-R will reliably predict NICU graduates that will receive an ASD diagnosis.

Experimental design: A retrospective chart review was conducted on 195 NICU graduates, of which 174 were included in the final analysis. The MCHAT-R was conducted at 16 months of age (corrected if premature). Exclusion criteria encompassed children with unknown diagnostic outcomes or those awaiting evaluation for ASD. A logistic regression model was used to evaluate potential associations between independent variables—such as multiple birth status, birth weight, gender, ethnicity, and M-CHAT-R screening results—and the dependent variable of an ASD diagnosis. Positive and negative predictive values were calculated to evaluate the diagnostic performance of MCHAT-R in identifying an ASD diagnosis.

Data and results: Of the 174 cases, 17 children have a diagnosis of ASD. There were 23 children had an elevated MCHAT-R and 11 of those children have an ASD diagnosis. The positive predictive value (PPV) was 47.8% and the negative predictive value was 96.2% (NPV). The logistical regression model showed significant association (p=.002) between a positive MCHAT-R and an ASD diagnosis. Children with a positive MCAT-R have 232.74 times higher odds of having an ASD diagnosis compared to those with a negative MCHAT-R. There was no association between multiple birth status, birth weight, gender, ethnicity and an ASD diagnosis.

Conclusion: Our findings support the validity of the MCHAT-R as a screening tool for ASD in the NICU graduate population. The PPV and NPV are similar to the accepted values for children that did not spend time in the NICU, suggesting that it is valid in this population. While we did not identify additional factors predictive of an eventual ASD diagnosis in this cohort, expanding the patient population in future studies may help uncover other potential indicators. The Bayley-4 developmental screener, introduced in 2019, offers the opportunity to stratify patients into risk categories and will be incorporated into future analyses as more data becomes available.

Overall, this study reinforces the MCHAT-R's utility as a valid ASD screening tool for NICU graduates but highlights the need for further research to explore additional predictive factors and refine screening approaches in this high-risk population.

CHARACTERIZING THE CLPC ADAPTOR PROTEINS MCSAB IN THE OBLIGATE INTRACELLULAR BACTERIUM, *CHLAMYDIA TRACHOMATIS*

Terry A. Wiese, Jeonghoon Lee, Shiomi Junker, Derek J. Fisher, Scot P. Ouellette (UNMC Omaha, NE)

Background, Significance, Hypothesis: *Chlamydia trachomatis* (*Ctr*) is an obligate intracellular, Gram-negative pathogen that is the leading cause of bacterially sexually transmitted infections and preventable infectious blindness worldwide. According to the CDC, *Ctr* is the most frequently reported notifiable sexually transmitted disease in the United States, particularly affecting women of reproductive age. If untreated, then *Ctr* infections can lead to severe complications, including pelvic inflammatory disease (PID), ectopic pregnancy, tubal infertility, and chronic pelvic pain. *Ctr* undergoes a unique biphasic developmental cycle, alternating between an infectious, non-replicating elementary body (EB) and a non-infectious, metabolically active replicating reticulate body (RB). This cycle relies on numerous proteases and protein complexes that regulate bacterial development, homeostasis, virulence, cell differentiation, and viability. In model organisms, caseinolytic protease (Clp) systems have been shown to play a central role in these processes. These systems are highly evolutionarily conserved and typically consist of an unfoldase, such as ClpC or ClpX, and a protease, such as ClpP. The unfoldase uses ATP to unfold substrates, directing them to the ClpP protease for degradation. In addition to the core Clp components, accessory proteins such as McsAB modulate substrate specificity. McsA acts as an adaptor protein, activating McsB, an arginine kinase that phosphorylates target substrates. These phosphorylated substrates are then recognized by the ClpCP system for degradation, facilitating proper bacterial development. Interestingly, despite its highly reduced genome, *Ctr* has retained ClpC and the McsAB adaptor proteins, which are commonly associated with Gram-positive bacteria and mycobacteria. As part of our ongoing research, we recently demonstrated that overexpression of the ClpC component accelerates chlamydial developmental progression. These findings suggest that targeting unique phosphorylated substrates of the ClpCP system could provide a foundation for novel anti-chlamydial therapies. As such, we hypothesize that McsAB functions as a phosphoarginine kinase, marking substrates essential for *Ctr* differentiation for degradation by the ClpCP system. In this model, McsAB acts as a key regulator, or “gatekeeper,” of chlamydial developmental progression. To investigate this, we have begun examining the role of McsAB in proteomic turnover and bacterial growth and development.

Experimental Design: To test our hypothesis, a series of *in vivo* experiments were conducted to characterize the functions of McsA and McsB. CRISPR interference (CRISPRi) was employed to achieve *mcsAB* knockdown whereas McsA and/or McsB were overexpressed. Both strategies rely on inducible expression systems. This was followed by indirect immunofluorescence assays (IFA) to visualize the effects of knockdown or overexpression on chlamydial growth and development. Inclusion forming unit (IFU) counts were used to quantify infectious progeny (i.e., EBs). Additionally, RT-qPCR was performed at multiple time points to evaluate the impact of *mcsAB* knockdown on the expression of other well-characterized transcriptional regulatory genes in *Chlamydia*.

Data and Results: Preliminary *in vivo* IFA data demonstrate that *mcsAB* knockdown significantly impacted chlamydial growth and development. This finding was further corroborated by IFU analyses, which revealed a significant reduction after *mcsAB* knockdown. RT-qPCR confirmed the effectiveness of the knockdown by showing significant differences in transcript levels between uninduced and induced conditions, with no off-target effects on other well-characterized developmental regulatory genes in *Chlamydia*.

In contrast, preliminary studies indicate that overexpression of McsA and/or McsB had no measurable impact on chlamydial growth, development, or biological significance. These findings were supported by both IFA and IFU data, as overexpression of any isoform tested exhibited no significant difference from its matched, uninduced control condition.

Conclusion: We propose that *Chlamydia* uniquely regulates ClpC substrate degradation by the McsAB system for timely and appropriate morphological changes needed for infection and replication.

THE EFFECT OF MARIJUANA USE ON AGE OF LUNG CANCER DIAGNOSIS: A RETROSPECTIVE STUDY

Ryan P. Kimball, Paul J. Wilkinson, Eric C. Lis, Ryan W. Walters, Jacqueline W. Poole
Creighton University School of Medicine, Omaha, NE

Background, Significance, Hypothesis:
Tobacco is the leading preventable cause of lung cancer, and both duration and quantity of tobacco smoking are positively correlated with risk of lung cancer. Marijuana smoke has many shared carcinogens with tobacco, including benzopyrene, benzanthracene, nitrosamines, phenols, aldehydes, and vinyl chlorides. Marijuana has long been speculated to increase the risk of developing lung cancer due to many shared carcinogens with tobacco and its ability to cause cancer cells to grow in vitro. While a potential synergistic carcinogenic effect of marijuana and nicotine has been suggested, no clinical studies have yet confirmed this. Given that the smoke of marijuana contains many shared carcinogens with tobacco, it was hypothesized that users of both inhalants would be diagnosed with lung cancer at a younger age than those who used tobacco alone.

Experimental Design:
The electronic medical record system EPIC was utilized to identify patient age at diagnosis and lung cancer stage at diagnosis in patients with biopsy-confirmed lung cancer in the CHI Health System (Omaha, NE) from January 1, 2017 to December 31, 2022. A total of 156 patients with a history of smoking both tobacco and marijuana concurrently met inclusion criteria. 135 patients with a history of smoking tobacco (but not marijuana) were matched as controls according to shared demographic data. One way analysis of variance (ANOVA) was used to compare age at diagnosis, whereas the chi-square test was used to compare stage at diagnosis.

Data and Results:
The average age at diagnosis of patients who smoked tobacco and marijuana was 61.3 ± 7.5, compared to 64.0 ± 7.8 for patients who smoked only tobacco (p-value = 0.041). Of patients who smoked tobacco and marijuana, 83 (53%) had stage III or IV lung cancer at time of diagnosis, compared to 75 (56%) patients who smoked only tobacco (p-value > 0.05). There was no significant difference in stage of lung cancer at time of diagnosis between those who smoked marijuana and tobacco vs those who smoked only tobacco (p-value = 0.205).

Conclusions
These results suggest that concurrent use of marijuana and tobacco is associated with a lower age at diagnosis of lung cancer compared to using tobacco alone. There was no difference in stage of cancer at diagnosis between those who smoked both agents compared to those who smoked tobacco alone. Along with the lack of previous studies, there are several limitations within this study that restrict adequate research on the effects of marijuana on lung cancer progression. These limitations include social limitations, such as patients not feeling comfortable sharing marijuana use, inconsistent clinical documentation of marijuana use, and the lack of standardization of marijuana use. The lack of standardization of marijuana use caused difficulty in the EMR quantification of marijuana use. While cigarette smoking has a standard unit in pack years, marijuana use is difficult for clinicians to quantify. Endorsements of marijuana use varied drastically among patients which provided difficulty in quantifying and correlating marijuana use with tobacco use. Further studies are needed to better quantify the risk associated with marijuana use and the effects of combination product use have on lung cancer progression.

REDUCED SURVIVAL IN LOW-INCOME PATIENTS WITH SOLITARY PLASMACYTOMA OF BONE: A RETROSPECTIVE COHORT ANALYSIS

Kate S. Woods, Mitchell A. Taylor, Peter T. Silberstein (Creighton University School of Medicine, Omaha, NE)

Background, Significance, Problem: Solitary plasmacytoma is a rare type of plasma cell dyscrasia characterized by a localized, clonal proliferation of malignant plasma cells. It is divided into two subtypes: extramedullary plasmacytoma, where plasma cells infiltrate soft tissue, and solitary plasmacytoma of bone (SPB), which involves a single bone lesion. Previous studies have investigated incidence rates and prognostic factors for patients with SPB, noting higher incidences in Black, male, and elderly patients. Key factors associated with improved overall survival in SPB patients include younger age, tumor size smaller than 5 cm, and fewer patient comorbidities. Additionally, a retrospective analysis using the National Cancer Database found significantly higher overall survival for SPB patients with private insurance, higher income, or those treated at academic medical centers. Given the influence of socioeconomic status and access to care on mortality, we sought to expand upon these findings through a population-based analysis on the effect of demographic factors, especially income, on disease-specific survival (DSS) in SPB patients, utilizing the Surveillance, Epidemiology, and End Results (SEER) database.

Experimental Design: The SEER database was queried to identify all patients diagnosed with biopsy-proven cases of solitary plasmacytoma of bone from 2000-2021. Annual income data from the SEER database was obtained from United States Census Bureau five-year estimates, and cohorts were stratified by low-income (< $74,999/year) and high-income (> $75,000/year). Statistical analysis was completed using SPSS version 29.0 and included Chi-squared, Kaplan-Meier and log-rank, and stepwise Cox regressions. Statistical significance was considered at $p<0.05$.

Results: The retrospective analysis revealed significant associations between annual income and disease stage ($p=0.021$) as well as chemotherapy treatment ($p=0.002$), where lower-income patients were diagnosed with higher rates of distant-stage disease (15.9% vs 12.8%) and required chemotherapy more frequently (21.7% vs 17.8%). Univariable Kaplan-Meier analysis revealed that higher-income patients had significantly improved mean survival (144.2 months) compared to their lower-income counterparts (135.3 months) ($p=0.006$). Stepwise multivariable analysis adjusting for age, sex, race and ethnicity, rural-urban living, primary tumor location, and disease stage revealed that a lower income was independently associated with an increased disease-specific mortality risk (aHR 1.19; 95% CI 1.04-1.37; $p=0.012$) compared to higher-income individuals.

Conclusion: This population-based study highlights disparities in outcomes for low-income patients diagnosed with SPB, demonstrating significantly lower DSS even after adjusting for potential confounders. These findings underscore the need for individualized treatment approaches for patients with lower socioeconomic status. Careful consideration should be given to low-income SPB patients due to their increased mortality risk. Future research and interventions should focus on improved early detection of SPB in this population to enhance outcomes. Overall, this study is consistent with prior literature demonstrating poorer overall survival in SPB patients with lower median household incomes. However, our population-based analysis expands upon these findings by commenting on DSS. Further, we offer a broader and more accurate representation of SPB prevalence, reducing some of the selection bias inherent in hospital-based registries.